Abrasion damage of concrete for hydraulic structures and mitigation measures: A comprehensive review

Qiong Liu [a,b], Lars Vabbersgaard Andersen [a], Mingzhong Zhang [b], Min Wu [a,*]

[a] Department of Civil and Architectural Engineering, Aarhus University, Aarhus 8000, Denmark
[b] Department of Civil, Environmental and Geomatic Engineering, University College London, London WC1E 6BT, UK

ABSTRACT

Abrasion damage of concrete induced by sediment-laden flow has been a significant durability problem for hydraulic structures. Due to the complexity of dynamic fields and concrete properties as well as the interaction effects between them, many aspects are still subjected to debate despite the tremendous efforts that have been made. In light of this and in order to further advance our understanding, this work aims to present a state-of-the-art review on critical aspects of the abrasion behavior of concrete. Important theoretical basics and mechanisms behind abrasion-induced concrete damage are presented first and different performance indicators that have been used for abrasion damage characterization are discussed. Following that, relevant abrasion test methods are comparatively reviewed and the effects of important hydraulic parameters and concrete properties on concrete abrasion behavior are analyzed in depth. Moreover, representative prediction models proposed for the estimation of concrete abrasion damage are discussed. In addition, an overview of recent development strategies for improving concrete abrasion resistance is presented. Based on the critical analysis of the research status, some important research gaps and challenges are highlighted.

1. Introduction

The abrasion damage of concrete for hydraulic structures is a physical process of continuous loss of material on the surface, mainly caused by hydrodynamic loads. Globally, there are a large number of hydraulic structures, e.g., various water-conveying tunnels, pipelines, and dams, which are being exposed to severe hydroabrasion/abrasion damage, as seen in Table 1. The excessive abrasion depth puts hydraulic concrete infrastructure operations at risk and leads to high maintenance costs, among others [1]. More seriously, the mega-failures of hydraulic concrete structures induced by long-term abrasion may endanger public safety. The abrasion damage accumulated in the long term or caused by significant flood disasters has been a critical concern for hydraulic concrete structures.

Therefore, comprehensive considerations must be given in the initial design stage to improve the abrasion resistance of such structures, in particular, for infrastructures that require a long service life. Among others, an optimized hydraulic design and operation regime, together with the selection of concrete materials, may substantially reduce concrete abrasion damage, and consequently the required maintenance and refurbishment costs. This will bring significant benefits for the

stakeholders of the facilities, e.g., in terms of safe operation and cost-effectiveness [8], and more generally for an overall sustainable society.

Hydroabrasion has been investigated for a few decades, and most studies have been developed based on laboratory tests [9–17]. However, in many cases, the obtained experimental outcomes vary considerably due to the absence of standardized test conditions and procedures. Besides, comprehensive evaluation and assessment of concrete abrasion damage are found to be lacking in most obtained results, typically as a consequence of limited influencing parameter data and weak external validity [18]. Furthermore, effective strategies for improving concrete abrasion resistance should be promoted so that durability performance can be ensured even if hydraulic structures are exposed to a harsh environment, e.g., high flow velocity and high sediment flux conditions. Various methods have been suggested in this regard, including, e.g., the use of discontinuous fibers, supplementary cementitious materials, ductile rubber particles, and coating materials [19–22].

Despite the great efforts that have been made in the research community, the fundamental mechanisms behind concrete abrasion damage have not been revealed comprehensively and durability designs of hydraulic structures concerning concrete abrasion damage are far from being resolved yet. Therefore, a state-of-the-art review on the abrasion

---

Table 1
Some field cases of concrete abrasion damage in hydraulic structures.

Ref.	Type of hydraulic structures	Location	Abrasion duration	Abrasion depth
[2]	Stilling basin of the Vrhovo HPP spillway	Slovenia	297 hours	0.2–0.8 mm
[3]	Coastal Stepped Revetment	UK	1 year	3.5–4.5 mm
[4]	Confederation Bridge	Canada	20 years	50 mm
[5]	Dam	US	-	Up to 3 m
[6]	Sediment bypass tunnel (Palagnedra)	Switzerland	-	Up to 2 m
[7]	Sediment bypass tunnel (Hintersand)	Switzerland	-	1–4 mm/year
[7]	Sediment bypass tunnel (Runcahez)	Switzerland	-	< 1.5 mm/year
[7]	Sediment bypass tunnel (Val d'Ambra)	Switzerland	-	3 mm/year
[7]	Sediment bypass tunnel (Asahi)	Japan	-	22 mm/year

behavior of concrete for hydraulic structures is highly desirable. To fill the gap, this review focuses on the mechanisms and physics behind concrete abrasion damage, test methods to measure and assess abrasion damage, abrasion prediction models, and the effects of governing hydraulic and concrete parameters as well as the thorough strategies to improve concrete abrasion resistance. Based on this, the remaining challenges in producing concrete with high abrasion resistance for hydraulic structures can be identified.

The contents of the work are structured as follows. In Section 2, the theoretical background related to concrete abrasion damage is introduced and discussed. In Section 3, typical laboratory and in-situ test methods are presented and analyzed, followed by the representative prediction models in Section 4. In Section 5, the effects of hydraulic parameters and relevant concrete properties on the concrete abrasion behavior are analyzed in depth. In Section 6, representative measures and strategies for increasing the abrasion resistance of concrete are critically reviewed. In Section 7, research gaps and perspectives are proposed and discussed. Finally, in Section 8, some conclusions are drawn based on the discussions. Ultimately, this work aims to shed light on the important aspects of concrete abrasion damage by reviewing the existing knowledge, thus providing a basis for designing durable hydraulic concrete structures.

2. Theoretical background

2.1. Flow dynamics

2.1.1. Regimes for sediment transport

The abrasion damage of concrete is governed by complicated interactions between the flow and concrete material among which the dynamics of the sediments transported in the flow contribute a lot [8]. The motion of sediment particles can be characterized by rolling or sliding, saltation, and suspension [23]. The rolling motion occurs when the sediment particles are transported in contact with the concrete surface. An increasing flow velocity leads to the saltation of sediment particles with the trajectory of the moving sediments hopping away from the concrete surface and then impacting it under vertical accelerations. According to the findings in [24], the excess weight of sediment particles is supported by continuing upward impulses imparted by currents of fluid turbulence. This phenomenon takes turbulence intensity into account for the initiation and development of the sediment suspension [6].

It should be noted that sediment transport conditions are not constant and even different transport modes are highly intermittent in nature [25]. As reported in [26,27], the critical Shields number was in the range of 0.002–0.100 for the transition from rolling to saltation.

According to Francis's definition sketch, when the hop length of the saltating particle is larger than 1000D (D is the mean grain diameter determined by the mean aperture of sieves), the suspension mode appears [28]. The velocity-based criterion described in Eq. (1) also implies the suspension threshold that the fluctuation of the vertical flow velocity component exceeds the terminal particle settling velocity [29]:

$$w^{'} > V_{s} \qquad (1)$$

where $w^{'}$ is the vertical flow velocity component, V_{s} is the terminal particle settling velocity.

The bound of transport modes can be comprehensively described as a function of the transport stage T^{*} which is defined as the ratio of the Shields parameter to the critical friction velocity (Eq. (2)) [30].

$$T^{*} = \left(\frac{U_{*}}{U_{*c}}\right)^{2} \qquad (2)$$

where U_{*} is the Shields parameter and U_{*c} is the critical friction velocity.

Based on the measured results in [7], the suspension probability of abrasive sediments could be up to 41% when the mean particle size was 6.3 mm and the mean flow velocity was 12 m/s. This means that almost half of the sediment particles are transported through suspension. However, it was reported in [6] that abrasive sediments were dominantly transported in saltation mode with minor parts in rolling mode and some small particles with a size of 5 mm in suspension mode under the low fluid velocity of 0.53 m/s. The inconsistency (or variety) of the reported findings in those researches may be attributed to the different experimental conditions regarding, e.g., the roughness of the flume bed, the particle size, the flow velocity, etc.

2.1.2. Energy conversion theory

As presented above, there may exist three sediment transport modes in the abrasion process. In the suspension mode, almost all the kinetic energy is used to transmit the sediment-laden flow. The kinetic energy of the rolling particles is orders of magnitude smaller than that of those in the saltation mode [6]. As for the saltation mode, some kinetic energy would be converted into fracture energy that causes the initiation of cracks and concrete abrasion damage [31]. According to the specification of the input kinetic energy U_{i}, it can be divided into three components, as shown in Fig. 1. In general, there is limited kinetic energy absorbed by the concrete material (U_{a}), while a large amount of input kinetic energy is used to rebound the sediment particles (U_{r}). Differential thermal expansion tends to cause concrete fracturing. However, thermal energy (U_{h}) generated due to the continuous impact actions of abrasive particles is limited under water conditions. As a result, the kinetic energy of the flow causing the concrete abrasion damage is determined by the flow velocity V_{p} and the total mass m of the sediment-laden flow within the abrasion duration.

2.2. Flow-concrete interaction

As discussed above, sediment particles in the suspension mode will not contact the concrete surface and thus there is no related mechanical behavior that can cause abrasion damage in this mode. As for the rolling mode, abrasive sediments abrade the top film of the concrete surface [33]. In addition, the mechanical stresses induced by the saltation of sediment particles are the prime culprits that eventually cause cracking and spalling of the concrete surface layer [1]. There are two different abrasion wear mechanisms involved in the saltation mode, namely, cutting wear and impact deformation. Cutting wear is mainly associated with the horizontal component of the impact force and impact deformation is mainly associated with the normal component of the impact force (Fig. 2(a) and (b)) [34]. Finnie [35] first proposed the concept that abrasive particles cut into the material, thus resulting in abrasion material loss. However, according to the investigations in [36], cutting
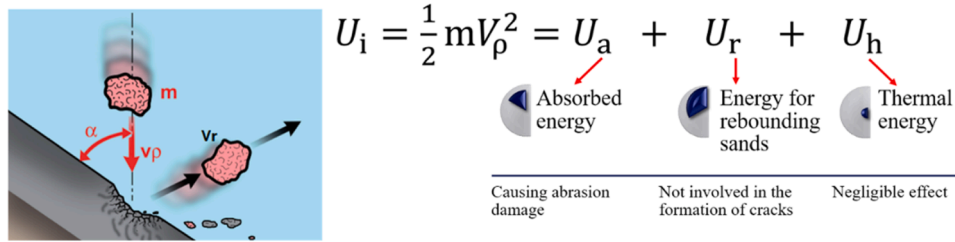
Fig. 1. Energy conversion theory.
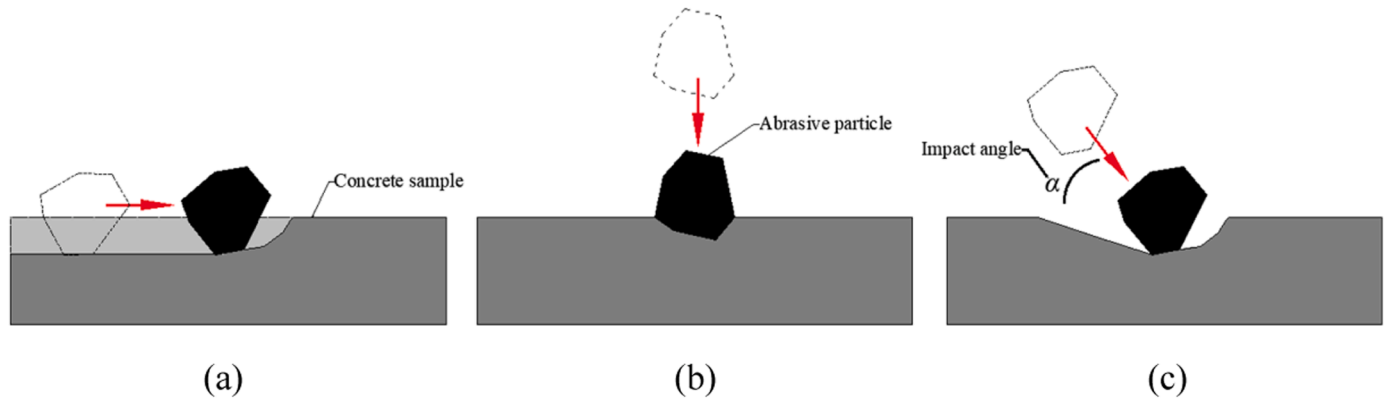Adapted from [32]

Fig. 2. Mechanical behavior: (a) cutting wear, (b) impact deformation, and (c) a combination of impact deformation and cutting wear [39].

wear has a minor effect on brittle materials. Then, Bitter supplemented the impact deformation mechanism to account for the abrasion damage caused by a normal attack [37]. In general, the material abrasion process is affected by a combination of force components parallel with the abrasion surface and normal to it when abrasive particles impact the concrete surface at a random angle (Fig. 2(c)). Consequently, abrasive particles not only dig into but also plow through surface layers, finally resulting in the material loss of concrete [38].

2.3. Abrasion damage evolution

2.3.1. Abrasion process

Essentially, the abrasion damage of concrete exposed to the sediment-laden flow may be considered as a progressive material loss process primarily induced by the mechanical degradation of concrete. According to the findings in [40], the chronological sequence of the abrasion damage progress of concrete includes the following stages:

(i) The motion of water causes pre-abrasion and the associated micro cracking. The micro-cracks initiate when the tensile strain arising from the deformation around the impact point exceeds the tensile strain capacity of concrete materials. With the loading time or the flow velocity increasing, intersecting micro cracks would accumulate and thereby cause the detachment of the eroded fragment on the top surface layer of mortar. Thus, the mortar contributes a lot to the concrete abrasion resistance in the first stage [36].

(ii) The repeated impacts of abrasive sediments carried by the water flow lead to penetrating cracks in the mortar matrix. Once such cracking appears, the flow tends to penetrate further into concrete and travel along interfacial cracks. More cement matrix will be destroyed, and some aggregates protruding out of the abrasion surface are subjected to the direct impact loads of the sediment-laden flow.

(iii) Some fine aggregates are taken out totally under the repeated impacts of the sediment-laden flow. This can be attributed to the fact that these fine aggregates with round, smooth, and small surfaces have less adherence to the cement matrix as compared with coarse aggregates [11]. As a result, tiny voids of the same aggregate size are generated in the concrete system which may cause undesirable cyclic effects on the crack development.

(iv) The total removal of aggregates may be followed once the abrasion of mortar reaches a certain depth comparable to the size of the aggregate [18]. As a consequence, a relatively rough abrasion surface may appear. In addition to the total removal of coarse aggregates, aggregate fracture may also occur in this stage when the large-size aggregates are subjected to super high-speed flow impacts.

2.3.2. Abrasion zones

The abrasion distribution zones of concrete may be divided according to the distance to the entry point of the sediment-laden flow, as shown in Fig. 3. The impact deformation contributes a lot to the abrasion
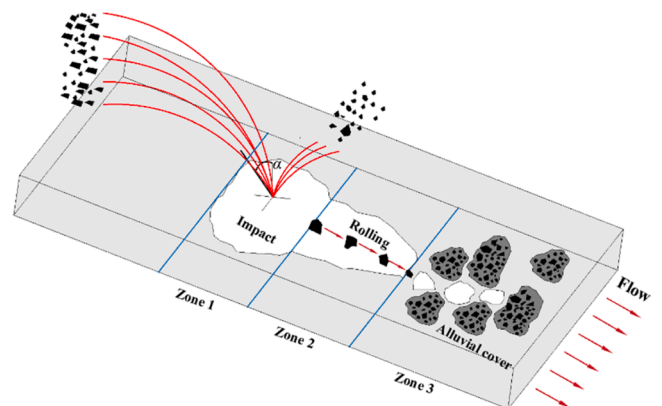

Fig. 3. Abrasion zones divided according to the distance to the entry point of the sediment-laden flow.

damage in Zone 1. Zone 2 is the middle zone where the scratching damage affects the most due to the rolling of abrasive particles. Zone 3 located in the flow downstream is partly or fully covered by sediments, where concrete is shielded from abrasion damage to some extent [6,36]. When the flow with low velocity cannot carry coarse sediments or the flow receives a relatively large supply of sediments (e.g., larger than its sediment transport capacity), some coarser sediments may stop on the concrete surface, thus forming an alluvial cover. In such a case, the minimum rate of concrete abrasion damage would be expected in Zone 3.

2.4. Quantification of abrasion damage

The quantification of abrasion damage is of considerable significance for the assessment of concrete abrasion damage. Abrasion damage characterization, including the mass/volume loss (rate), abrasion depths as well as depth distributions, and the affected areas, would be significant performance parameters to quantitatively compare and analyze the

abrasion damage phenomena.

Concrete mass loss or relative mass loss rate (that is the mass loss divided by the loading duration or the initial mass of the sample) is among the most frequently used parameters to characterize abrasion damage [41] since it can be obtained rather easily by weighing the mass before and after abrasion tests. However, there exist limitations in quantifying concrete abrasion damage through mass-loss related parameters due to the variation in concrete density for different mixtures, among others.

Volume loss may be a good indicator to quantify the abrasion damage of concrete with various densities [10,11]. Such an indicator for quantifying the material volume loss is calculated based on the known density of the concrete mixture and mass loss measurement [42]. In those standard abrasion tests (see Table 2), the volume loss is defined according to the volume of the specimen before and after abrasion tests, whereas the volume is calculated based on the real mass in the air and the apparent mass when suspended in the water [10]. Besides, the abraded volume can also be determined by the volume of the non-stick

Table 2
Summary and comparison analysis of different abrasion test methods.

Method		Type	Measurement	Advantage	Disadvantage	Application
Standard	ASTM C418 [9]	Sandblasting test methods	Ratio of volume loss and abrasion area	• It simulates the action of abrasive sands. • Controllable for the severity of the abrasion damage.	• The abrasive sands are generally of small size. • The abrasive sands are not transported by water but by high-pressure air.	• Evaluate the abrasive resistance of concrete for hydraulic structures
	ASTM C779 [44]	(1) Revolving-disk methods (2) Dressing-wheel methods (3) Ball-bearing methods	Abrasion depth	• Testing procedures differ in the type and degree of the abrasive force. • Shorten the testing time and accelerate the reflection of concrete abrasion damage.	• The test procedures are performed without water which leads to low similarity to the actual field conditions. • Only mechanisms of dry friction can be simulated. • Sufficient abrasion may not be achieved.	• Measure the abrasion resistance of concrete for pavements and floors
	ASTM C944 [45]	Rotating-cutter methods	Abrasion depth or mass loss	• Suitable and efficient for estimating abrasion damage of highway and bridge concrete mainly subjected to compression loads.	• Only grooving caused by dry friction can be simulated. • Not representative of hydroabrasion.	• Estimate the abrasion resistance of concrete for highways and bridges
	ASTM C1138 [10]	Underwater steel ball methods	Mass loss or mass loss rate	• Suitable for studying abrasion induced by sediment rolling, sliding, and impacting. • Eliminate the need to use large and long water channels and reduce the experimental costs.	• There exist evident shape differences between steel balls and waterborne particles. • The testing time of 72 hours for a single abrasion test is too long.	• Evaluate the abrasion resistance of concrete for hydraulic structures
Disk grinding [46,47]		(1) Böhme abrasion test methods (2) Wide disc test methods	Mass loss, volume loss, abrasion depth	• Suitable for studying abrasion induced by grinding	• The testing procedure is not representative of hydroabrasion. • The testing time is long.	• Estimate the abrasion resistance of concrete for roads and highways
Waterborne sand impact [17,19,40,48,49]			Mass loss, volume loss, abrasion depth, or abrasion rate	• High similarity to the field flow environment. • Multiple abrasion mechanisms including impacting deformation, cutting wear, and sliding scratching can be revealed.	• It is hard to achieve the desired sediment content and ensure the homogeneity of the sediment-laden flow. • The robustness, i.e. various and complex flow conditions (e.g., flow velocity, abrasive shape, and sediment contents) may be limited.	• Evaluate the abrasion resistance of concrete for hydraulic structures
High-pressure hydro-abrasive jet [11,50,51]			Mass loss, volume loss, abrasion depth, or abrasion rate	• Accelerate the abrasion process through high-speed flow. • Effective in testing the relative abrasion resistance of different concrete mixtures.	• Stress concentration may occur due to the water jet with high pressure acting on a small surface area. • The flow velocity under high pressure is larger than that in the field.	• Evaluate the abrasion resistance of concrete for hydraulic structures
Scaled physical-model [6,8,52,53]			Abrasion depth	• High similarity to the field conditions. • Advanced data recording system.	• The transferability of the results obtained from scaled physical-model tests to field applications is difficult, due to potential scale effects.	• Evaluate the abrasion resistance of concrete for hydraulic structures
In-situ abrasion [15,16]			Abrasion depth	• Accurate abrasion damage data.	• Field measurement for hydraulic structures is challenging. • In-situ tests are not cost-effective.	-

plastic material that is filled in the abrasion crater [43]. One common issue of using mass- and volume-loss related parameters is that the results are normally expressed as the average of the entire tested samples, which cannot demonstrate an important characteristic, namely the distribution of abrasion damage on the concrete surfaces.

Abrasion depths are another important variable to characterize concrete abrasion damage. Since it can be measured at different spots, the results may be used to reflect the distribution of abrasion damage. However, accurate measurement of abrasion depths may be a challenging task, as the abrasion depth is rather shallow in most cases. According to the experimental investigations in [54], abrasion depths seem to distribute unevenly on the abrasion surface area and thus abraded concrete surfaces appear rugged, which also makes the measurement process more complex. As reported in [55], abrasion depths are mostly defined as the average or the maximum value, i.e., based on the measurement of a single or only a few spots on the abrasion surface using a digital dial gauge [41]. The depth penetration can also be measured using transducers, which is especially relevant when the penetration on the concrete surface is slight [56]. In addition, the WMP ECLIPSE CNC machine was used by Horszczaruk [20] to measure the decreased height of the concrete surface with a maximum resolution of 0.01 mm. It is of interest to highlight that the methods based on three-dimensional (3D) scanners outperform most other measurement techniques due to the ability to capture the morphology of the concrete abraded surface and evaluate the abrasion depth accurately. Apart from the abrasion depths, the abrasion area distributions corresponding to different abrasion depth intervals can also be obtained from the abrasion morphology [54]. In addition, the abrasion width or length as an indirect measurement can also be used to determine the abrasion area from the cross sections [48]. Such information is very relevant for analyzing concrete abrasion damage and predicting the long-term effects.

3. Abrasion test and damage quantification methods

The main abrasion test methods available are listed in Table 2, among which the most typical ones are illustrated in Fig. 4. The standard test method ASTM C1138 [10] is a representative one for evaluating the relative abrasion resistance of concrete. Besides, waterborne sand impact methods are also widely used to simulate the concrete abrasion behavior [17,19,48,49], and high-pressure hydro-abrasive jet methods are used to test the effects of high-speed flow [11]. In addition, scaled physical-model test methods provide close similarity to the field conditions [6]. The above test methods reproduce the typical forces with varied successes to simulate concrete abrasion damage. However, due to the complexity and variety of hydraulic conditions, the obtained outcomes from laboratory tests appear to vary considerably, and therefore, the relevance of the obtained laboratory results is questionable regarding the real-world scenario. Last but not least, in-situ tests have also been adopted, which provide results from the field directly [15,16].

3.1. Standard test methods

The US standard test methods are widely used to investigate concrete abrasion behavior including ASTM C418 [9], ASTM C779 [44], ASTM C944 [45], and ASTM C1138 [10]. The ASTM C418 method simulates concrete surface abrasion based on the sandblasting procedure. For the ASTM C779 method [44], three types of abrasion test machines are involved including the revolving-disk machine, dressing-wheel machine, and ball-bearing machine, mainly simulating cutting actions of abrasive tools. The ASTM C944 method suggests the use of a rotating cutter and a drill press to consider the rubbing and grinding stresses. Different from the above three tests under dry abrasion conditions, the ASTM C1138 tests are performed underwater using steel balls to simulate actions of waterborne particles (see Fig. 4(a)). As seen in Table 2, main performance indicators, e.g., abrasion depth and mass loss-related parameters are used to estimate scuffing damage on the surface and

abrasion material loss. Despite the ease of use for these standard test methods, their application to complex hydraulic conditions is questionable due to the low similarity to the field flow conditions.

3.2. Disk grinding test methods

The Böhme abrasion test methods are widely used in EU countries to assess concrete abrasion damage. In the testing procedure, the steel grinding disk is placed horizontally and made to rotate with the abrasive (20 g of corundum powder) spreading on the surface. After a series of turns of the Böhme disk, the surface of the concrete is ground due to the friction. Generally, the Böhme abrasion test is performed in dry conditions [46]. However, according to the testing procedure in [57], approx. 13 ml of water (i.e. 180–200 droplets) per minute is poured on the test track to develop wet conditions. Similarly, "the wide disc test" described in the EN 1338 standard [47] can also be used to consider grinding wear of concrete using corundum (white fused alumina) as the abrasive agent and vertically placed rotating-disk as the abrasive tool. Main performance indicators, i.e., abrasion depth and mass or volume loss-related parameters can be used to assess grinding damage on the concrete surface.

3.3. Waterborne sand impact methods

Waterborne sand impact methods are also widely used for the determination of the abrasion resistance of concrete [17,19,49]. The waterborne sands, which are mostly quartz sands acting as abrasives in the case of laboratory experiments, are mixed with pure water to form the sediment-laden flow. The circulating sediment-laden flow typically powered by a pump in the test system continuously impacts the concrete surface at a designated constant speed, and finally leads to abrasion wear under long-term repeated loading, as seen in Fig. 4(b) [58]. The waterborne sand impact methods yield almost the realistic concrete abrasion conditions that occur in the field and provide a comprehensive assessment of abrasion damage based on various performance indicators, e.g., mass loss, volume loss, abrasion depth, and abrasion rate, as seen in Table 2. Various abrasion mechanisms including impacting deformation, cutting wear, and sliding scratching can be revealed. Thus, the similarity between laboratory conditions and field environments is a great advantage, but the robustness and reliability of the methods under various and complex flow conditions may be limited in some cases due to potential constraints in creating the desired conditions and rather expensive experimental costs.

3.4. High-pressure hydro-abrasive jet methods

The kinetic erosion by the high-speed flow has a significant impact on the abrasion process of concrete. Generally, abrasion damage induced by the high-speed flow is simulated by high-pressure water jet methods [11,50,51]. As seen in Table 2, this method can accelerate the abrasion damage and shorten the time needed to differentiate the abrasion-resistant performance of different concrete mixtures [59]. Similar to waterborne sand impact methods, the abrasion damage obtained through high-pressure hydro-abrasive jet methods can also be comprehensively assessed based on various performance indicators. However, the generated abrasion damage is highly associated with the stress concentration phenomenon. This is because the water jet exported from the small size nozzle typically possesses a considerably high pressure and acts on the small surface area, as shown in Fig. 4(c) [60]. Even though the methods are effective in testing the relative concrete abrasion resistance, the link between the obtained experimental results and those from the field tests is rather difficult to establish.

3.5. Scaled physical-model test methods

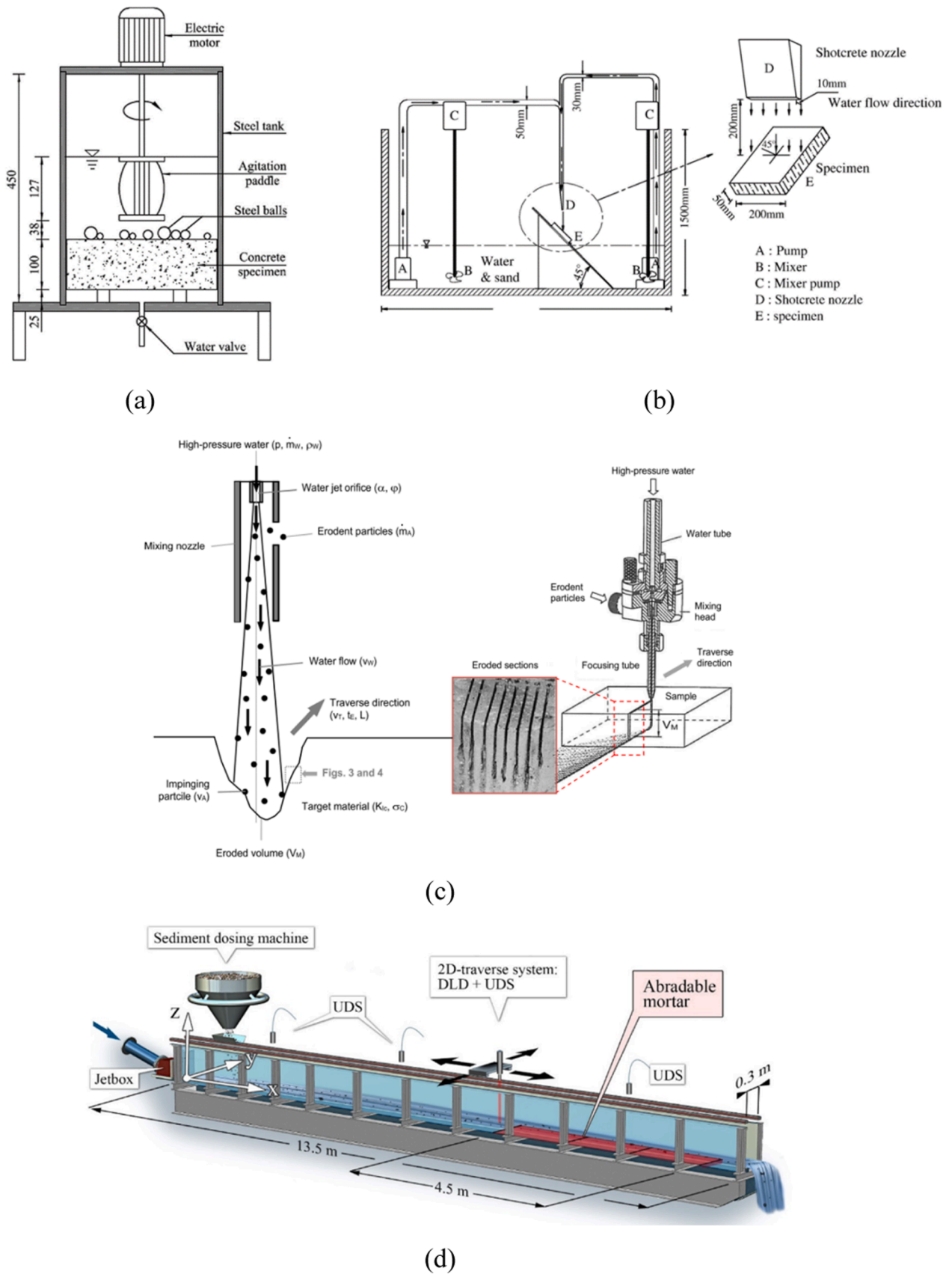Although the methods introduced in Sections 3.1.1 to 3.1.3 can be

Fig. 4. Typical abrasion test methods: (a) ASTM C1138 methods [10], (b) waterborne sand impact methods [40], (c) high-pressure hydro-abrasive jet methods [11], and (d) scaled physical-model test methods [6].

applied to study the abrasion behavior of concrete to different extents, the results measured at a laboratory scale may be less representative for the reality [61]. It is known that the applicability of the laboratory methods for assessing the abrasion behavior of the concrete can only be achieved by performing tests under lab conditions very similar to those in the actual operating hydraulic environment, including most (if not all) of the relevant hydraulic and hydrological parameters [62]. Based on this, the scaled physical-model test methods are desirable to investigate the concrete abrasion behavior of hydraulic structures [12,13,63]. Auel [6] studied the relation between the flow parameters and the abrasion behavior of concrete in a scaled sediment bypass tunnel model where Laser-Doppler-Anemometry (LDA) was applied for the measurement of instantaneous flow velocities and concrete abrasion depth, as seen in Fig. 4(d). However, in some cases, the recorded abrasion depth was less than 0.25 mm beyond the range of the laser accuracy. Despite the fact that it is a scaled test model, the costs are pretty high. Besides, the model calibration for the field application could be another problem because of complex hydraulic conditions and challenges to obtaining accurate results from in-situ investigations. Last but not least, the transferability of the results to field applications is difficult due to potential scale effects.

3.6. In-situ abrasion test methods

In-situ abrasion tests can provide accurate abrasion data in the field but they are rarely carried out due to the huge costs and, more importantly, the accessibility to relevant sites. Kryžanowski et al. [15] analyzed the abrasion damage of concrete linings located at the lower Sava River in the southeast of Slovenia. The concrete structures were exposed to suspended sediment-laden flow, so the dominant abrasion mechanism was grinding rather than impacting. As mentioned in Table 2, the average abrasion depth was used to assess concrete abrasion damage. However, the abrasion surface was rough due to the fluctuation of the water current. Thus, there was a measuring precision of $\pm 10^{-4}$ m for different observation points, which gave rise to doubt about the reliability of the measurement. Additionally, a field test site selected by Jacobs et al. [16] was the Runcahez sediment bypass tunnel located in the Swiss Alps. Sediment flux was always accumulated in the channel center, thus leading to the inaccuracy in the observed abrasion patterns.

To sum up, it should be noted that there are no single tests that can adequately assess the abrasion resistance of concrete for hydraulic structures under all possible conditions. Another important point to be mentioned is that the similarity or relevance between the laboratory tests and field conditions is poor because the natural field conditions are rather robust and complex. The reliability and representativeness of laboratory methods for exploring a complex physical phenomenon are largely dependent upon their ability to adequately simulate the actual conditions.

4. Abrasion prediction models

Durability design and service life assessment of hydraulic concrete structures are generally based on concrete abrasion prediction models. Different models have been proposed to investigate and predict the abrasion damage of concrete, including empirical models, semi-empirical models, probability-based statistical models, and models based on machine learning methodologies.

4.1. Empirical models

Empirical models are widely used to predict concrete abrasion due to the ease of access to experimental data. At present, the most widely used models show a proportional relation between concrete abrasion depth and its compressive strength [64–67]. With the variations of water-cement ratio, fly ash and rubber incorporation, and abrasion loading time, linear, polynomial, logarithmic, and powder functions

have been applied to predict concrete abrasion depth.

In some empirical models, concrete tensile and flexural strength, abrasion duration, and flow velocity are taken as independent variables to quantify concrete abrasion, e.g., mass loss and abrasion rates [68–71]. Based on all of the above discussions, the classification and framework of empirical models can be summarized in Table 3.

The empirical models are effective in characterizing the relation between abrasion material loss and governing influential parameters [40,41,65]. However, it is found that only one parameter is considered as a variable in the models while other influential parameters are considered in the constant coefficient. Consequently, the applicability of those models is questionable. This is because the wide variation in influential factors (hydraulic conditions and concrete properties) makes it unlikely that a single set of parameters can describe adequately the dependence of abrasive wear on any influence parameter.

4.2. Semi-empirical models

The accuracy of the prediction models may be improved using more advanced methods, e.g., semi-empirical models, developed based on a combination of experimental measurements and mathematical theories. As mentioned in Section 2.1.2, energy conversion is involved in the abrasion process. Based on this, a formulation derived expressing abrasion as a function of kinetic energy was proposed by Bitter [37], as given by Eq. (3). However, only wear due to repeated impact deformation is considered in this model. This is inconsistent with the discussion in Section 2.2 that two forms of abrasion mechanical behavior, namely impact deformation and cutting wear, may exist simultaneously. On the basis of Bitter's model, a modified model was proposed that can consider the impact loads and account for the cutting effects of abrasive particles, expressed as Eq. (4) [72,73].

$$W_D = \frac{1}{2} \frac{M(V\sin\alpha - K)^2}{\varepsilon} \tag{3}$$

$$W = W_D + W_C = \frac{\frac{1}{2}M(V\sin\alpha - K)^2}{\varepsilon} + \frac{\frac{1}{2}MV^2\cos^2\alpha\sin2\alpha}{\varphi} \tag{4}$$

where W is the total volume loss caused by abrasion wear at the impacting angle of α and flow velocity of V, W_D and W_C are the abrasion wear caused by normal impact deformation and tangential cutting action, ε and φ are the contributing factors of kinetic energy associated with the impact deformation and cutting wear, M is the total mass of the sediment-laden flow within the loading duration, K is the critical velocity component normal to the concrete surface below which no

Table 3
The framework of existing empirical models. [40,41,65,66–71].

Empirical model	Format	Relation
Linear	$W_{ar} = af_c + b$	Relation between abrasion rates W_{ar} and concrete compressive strength f_c [40]
	$D = at$	Relation between wear depth D and abrasion time t [41]
Polynomial	$D = a_1 + a_2f_c + a_3f_c^2$	Relation between wear depth D and concrete compressive strength f_c [65]
	$M_l = a_1 + a_2f_{f/t} + a_3f_{f/t}^2$	Relation between mass loss M_l and concrete flexural or tensile strength $f_{f/t}$ [68]
Exponential	$M_l = e^{af_c}$	Relation between mass loss M_l and concrete compressive strength f_c [41]
Logarithmic	$D = a + b\ln f_c$	Relation between wear depth D and concrete compressive strength f_c [67]
Power	$D = af_c^b$	Relation between wear depth D and concrete compressive strength f_c [66]
	$W_{ar} = av^b$	Relation between abrasion rates W_{ar} and flow velocity v [69–71]

abrasion occurs, and the expression $\sin 2\alpha$ is chosen for data fitting without mechanistic significance behind it.

Ishibashi [74] proposed a prediction model based on flume experiments operated at supercritical flow conditions. The model also consists of a kinetic energy term accounting for the impact actions of the flow and a friction work term accounting for the cutting stresses of the flow, as indicated by Eq. (5). It is found that the latter term considers cutting abrasion wear to be a multiple compared to its kinetic term according to Eqs. (6) and (7). This is inconsistent with the discussion in Section 2.1.1 that most abrasive particles are transported in saltation mode and thus impact deformation is the dominant abrasion condition. Besides, the material properties of the flume bed in Ishibashi's model are considered in the coefficients C_1 and C_2 whereas only one group of coefficients is provided for concrete materials. In such a case, the variation in concrete performance cannot be considered in the model.

$$V_a = C_1 E_k + C_2 W_f \tag{5}$$

$$E_k = 1.5 V_{ts} \sum E_i N_i n_i \tag{6}$$

$$W_f = 5.513 \mu_d V_{ts} \sum \left(\frac{U_p}{W_{im}} \right) E_i N_i n_i \tag{7}$$

where V_a is the abraded invert volume, E_k is the total kinetic energy transmitted by saltation particles and W_f is the total friction work induced by grinding particles, C_1 and C_2 are material property constants, E_i is the energy transmitted by a single particle, N_i is the impact frequency within the total invert length, n_i is the amount of particles per unit of sediment volume, μ_d is the dynamic friction coefficient and V_{ts} is the amount of transported sediment over a certain period, U_p is the horizontal velocity component of the particle, and W_{im} is the vertical velocity component of the particle.

Some researchers demonstrated that the marginal influence of cutting wear was investigated on brittle materials (e.g., concrete and bedrock), especially when exposed to flow with rounded grains as present in river systems [75].

As a result, Sklar proposed a model mainly focusing on the impact wear. The basic form of the model is defined as below:

$$E = V_i I_r F_e \tag{8}$$

where E is bedrock abrasion rates, V_i is the average volume of rock detached per impact, I_r is the frequency of particle impacts per unit area per unit time, and F_e is the fraction of the river bed exposed to the flow.

Furthermore, the model can be simplified in terms of the shear stress, as shown below:

$$E = \frac{q_s w_{si}^2 Y}{L_S k_v \sigma_T^2} \left(1 - \frac{q_s}{q_t}\right) \tag{9}$$

where q_s is the sediment supply per unit width, w_{si} is the vertical component of the particle velocity, Y is Young's modulus, L_S is the total hop length, k_v is related to the conversion efficiency of kinetic energy from impinging particles to the inverted material (the suggested value $k_v = 10^6$ for bedrock as well as concrete), σ_T is the tensile yield strength of the rock, and q_t is the sediment mass transport capacity per unit width.

4.3. Probability-based statistical model

A probability-based statistical model for predicting abrasion wear of concrete was proposed by Dandapat and Deb [18]. In the probability-based statistical model, the sediment-laden flow is defined as the continuous flow layers arriving on the concrete surface. Based on such an assumption, the total abrasion mass loss can be calculated by accumulating the damage from all sublayers. The detailed expression of the model is given by Eqs. (10) and (11). The probability-based statistical model mainly focuses on the effects of mesoscale geometry of

aggregates on concrete abrasion damage without taking the influences of other key parameters (e.g., flow characteristics and other concrete properties) into account. Therefore, the lack of comprehensive analyses on various influencing parameters may limit its application.

$$M_{eroded}(t) = \sum_{i=1}^{n_g} \left(M_{exposed}^{total} \right)^i \times \rho_i \tag{10}$$

where $M_{eroded}(t)$ is the eroded mass induced by one layer action at any time t, $\left(M_{exposed}^{total} \right)^i$ is the total mass of aggregates in the exposed area, ρ_i is the distribution of the conditional probability, and i is the i_{th} sediment-laden flow layer.

$$M_{eroded}^{layer} = \int_0^T M_{eroded}(t) dt \tag{11}$$

where M_{eroded}^{layer} is the total eroded mass over the total abrasion duration T.

4.4. Models based on machine learning

The prediction models established based on machine learning methodologies may greatly improve prediction accuracy and ensure applicability to more general conditions. Gencel et al. [76] established models to consider the effects of aggregate contents, cement contents, and external load conditions on concrete abrasion behavior. The obtained results showed that models established based on machine learning methodologies exhibited better prediction performance as compared with general linear models. However, the prediction accuracy of models may be compromised due to a small database (about 50 data points). Ghafoori et al. [77] built prediction models based on machine learning methodologies using the data points obtained from ASTM C779 tests. Similarly, Malazdrewicz and Sadowski [78,79] established models based on experimental records of ASTM C944 tests. In [80], two machine learning methodologies, i.e. random forests (RFs) and artificial neural networks (ANNs), were adopted to predict concrete abrasion depth based on 690 experimental data points, where 12 influencing parameters were considered to account for the complexity of the abrasion damage for hydraulic concrete structures. It should be noted that some of the reported models can effectively predict concrete abrasion damage. However, for those models established on a small data set from a specific case study, their applicability under other complicated field conditions seems to be less convincing. Consequently, a large data set is desirable for models established based on machine learning methodologies.

5. Factors influencing concrete abrasion damage

5.1. Environmental conditions

5.1.1. Abrasion time

Concrete abrasion damage is a cumulative process of material loss, indicating a close relation to the abrasion loading time. In general, only when the micro-cracks are developed to be interconnected with the abrasion duration extending and the mortar layer peels away gradually, the erosion process can be investigated. Fig. 5 shows the variation of concrete abrasion depth over abrasion loading duration under different experimental conditions. It is found that the abrasion depth of concrete can be described as an approximately linear function of the abrasion loading time [41,55,64,67,78,81–85]. However, under different experimental conditions, the linear relationship appears to vary significantly. This can be illustrated by the comparison of abrasion depth at the loading time of 60 minutes where the largest abrasion depth of 2.85 mm and the smallest abrasion depth of about 0.43 mm can be investigated simultaneously [41,85]. Besides, it is found that the abrasion depth of concrete exposed to the flow for 20 minutes is 2.1 mm [84], which is
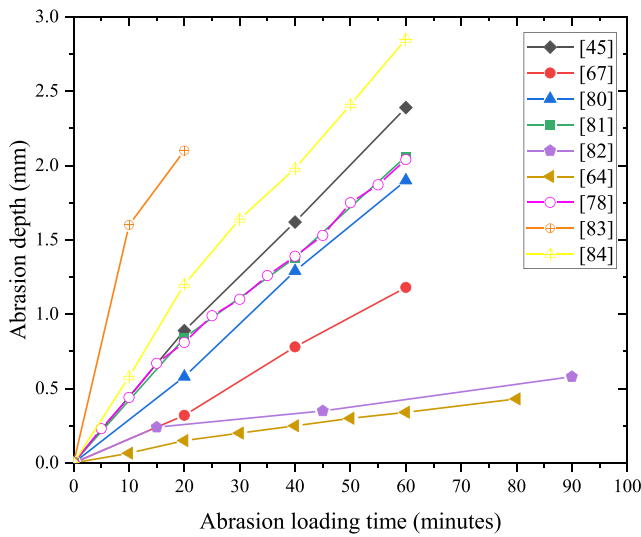
Fig. 5. Relation between the abrasion loading time and concrete abrasion depth.

Fig. 6. The relation between the flow velocity and the abrasion mass loss [54, 48,60,69,70,88,89].

close to the abrasion depth value of concrete under 60-minute loading [78]. This can be explained by the low W/B ratio for concrete mixtures in [78], thus leading to higher abrasion resistance.

Hocheng and Weng [50] reported the linear correlation between the abrasion loading time and the concrete mass loss at the flow velocity of 30 m/s [86]. Momber and Kovacevic examined the effects of abrasion time on the abrasion material loss at the high velocity of 253 m/s but in a short exposure duration of 1 s. The non-linear correlation between the abrasion loading time and mass loss was developed. The slow growth of abrasion mass loss was investigated at the later loading stage [60]. This can be explained by the abrasion process as introduced in Section 2.3.1. The top layer mortar is easily abraded away at super-high velocity loading, after which aggregates with high abrasion resistance are exposed, thus leading to the reduction in abrasion mass loss. Besides, it is found that there exists a lower limit of the loading time beyond which concrete abrasion damage appears. According to the theory in [60,87], the critical loading time can be defined as the ratio of a certain critical crack length to the cracking velocity.

$$t_c = l_{cr}/v_{cr} \tag{12}$$

where t_c is the critical loading time, l_{cr} is the critical crack length, and v_{cr} is the cracking velocity of the material. The cracking velocity of concrete can be estimated according to [87]

$$v_{cr} = 0.25\sqrt{E_m/\rho_m} \tag{13}$$

where E_m is the Young's modulus of the concrete material, and ρ_m is the concrete density.

Based on the proportionality model between applied energy and surface generation, the critical crack length can be found as

$$l_{cr} = \sqrt{0.5S_e} \tag{14}$$

where S_e is the surface area of abrasion material that can be estimated through graphical and numerical methods [60].

5.1.2. Flow velocity

Flow velocity is one of the critical parameters significantly affecting concrete abrasion damage. In terms of the influence of the flow velocity on the abrasion mass loss of concrete, some data published in the literature are summarized, as presented in Fig. 6 [54,48,60,69,70,88, 89]. According to the results in [11,54,65], when the flow velocity ranged from 2.5 m/s to 10 m/s, the measured mass loss of concrete
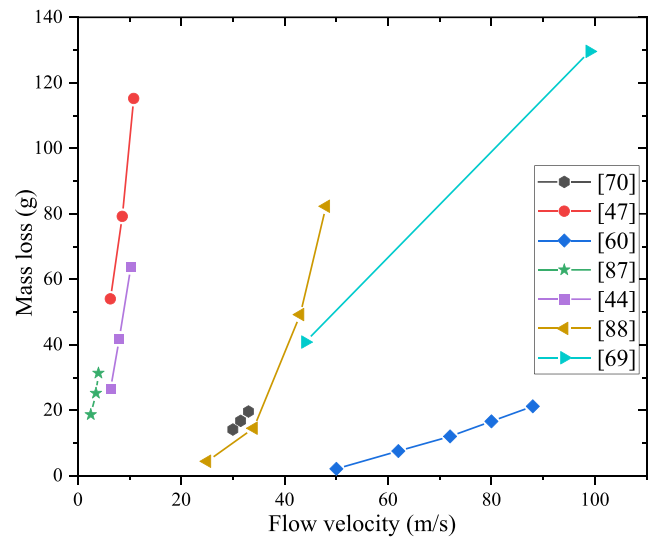
increased greatly from 18.7 g to 115.2 g. The rising trend of abrasion mass loss can also be investigated when concrete is exposed to the flow with a higher velocity ranging from 20 m/s to 100 m/s. However, the influence of high-speed flow loads on abrasion mass loss appears to vary considerably. A slight increase in the mass loss from 2.1 g to 21.2 g was reported in [68] when concrete was operated at super high-speed flow conditions of over 50 m/s. Overall, increasing the flow velocity leads to increased abrasion damage. According to the energy conversion theory (as introduced in Section 2.1.2), high-speed flow indicates high kinetic energy transferred to the concrete surface area [48,54]. The energy exerted on the concrete would convert into the fracture energy that leads to the formation and propagation of cracks, followed by abrasion material loss of concrete under abrasion loading.

In addition, there may exist a threshold velocity below which the kinetic energy is not large enough to drive the development of cracks, and hence the abrasion process is not induced [36]. Besides, the influence of the flow velocity on the abrasion mass loss of concrete can also be explained in terms of the sediment transport capacity of the flow [90]. At a relatively small flow velocity, the sediments may be settled. In this case, only a small portion of fine sediment particles can be transported as abrasives to cause abrasion damage, whereas the large-size particles may settle down on the surface and form a cover layer thus protecting the underneath concrete surface from abrasion damage, as described in Fig. 3. When the flow velocity reaches a level that can drive large sediment particles rolling or hopping, the abrasion rates tend to increase correspondingly [91]. As mentioned in Section 2.1.1, the increasing flow velocity may result in the shifts of the transport mode from rolling to saltation, and further to suspension. Consequently, an increase in the saltation hop length may occur, thereby leading to the reduction of the transmitted energy and less abrasion material loss [8].

5.1.3. Sediment content

The contents of abrasive sediments also influence concrete abrasion rates due to their abrasive tool effects mentioned earlier [92]. As shown in Fig. 7, the relation between abrasion rates and abrasive sediment contents (5%, 11%, 18%, and 25%) is approximately linear [71]. The effects of sediment contents vary with the change in the flow velocity. When the flow velocity is higher (114–135 m/s and 140–165 m/s), abrasion rates increase by 203% and 391% with the sediment contents increasing from 5% to 25%. However, a slight increase in abrasion rates can be investigated at the flow velocity of 57–61 m/s and 80–96 m/s. This is because the transporting capacity of the flow at the lower velocity
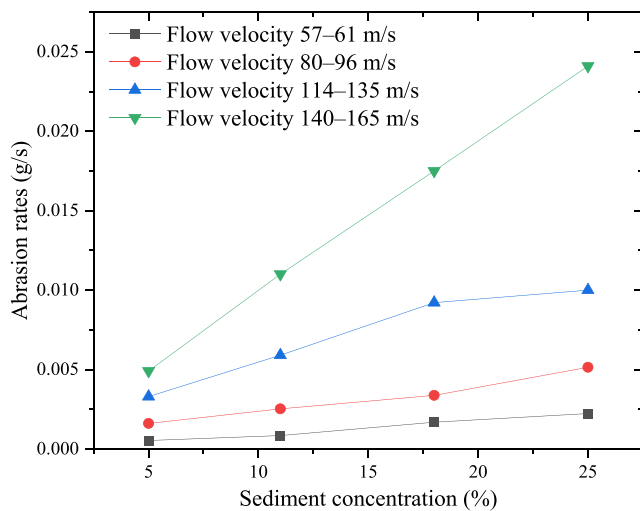
Fig. 7. The effects of sediment concentration on abrasion rates [71].

Fig. 8. Relation between the impact angle and concrete abrasion damage described by different performance indicators [48].

is smaller. As a result, less abrasive sediments are transported in the flow and less abrasion material loss occurs [93]. Sklar and Dietrich [94] developed theoretical analyses on the influences of the sediment supply, and results indicated that the abrasion rates exhibited a similar increasing trend with the increase of the sediment contents. However, the effects of sediment contents are too complex to fit into a linear coefficient.

Theoretically, the hydrodynamic loading can be assumed as a fatigue loading process. With the sediment contents increasing, the number of fatigue loading cycles increases and thus abrasion rates increase as well. From the perspective of energy conversion, the kinetic energy exerted on the concrete depends on the mass of the flow [86]. Accordingly, abrasion rates increase with the mass of transported sediments increasing. On the other hand, the abrasive sediment contents can affect concrete abrasion damage by limiting the exposure extent of the concrete to the flow [92]. The abrasion rates may peak at an intermediate level of the sediment transport rates due to the burial of the concrete by transient sediment deposits (see Section 2.3.2). Such a case occurs especially when the low-speed flow cannot carry the sediment particles or high-volume sediments are supplied to the flow [95]. As a result, some sediment particles would rest on the concrete to form a cover layer and thereby reduce the exposure extent of concrete to the flow, finally leading to a reduction in concrete abrasion rates. Besides, the presence of the slurry layer could affect the motion of coarse aggregates in the flow and further reduce their friction on concrete materials, thereby decreasing the abrasion damage induced by coarse aggregates [96].

5.1.4. Flow impact angle

The flow impact angle (α as shown in Fig. 3) is another important parameter affecting concrete abrasion. Many researchers have explored the relation between concrete abrasion rates and the impact angle [48, 97,98]. According to the findings in [97], the smallest abrasion rates occurred at the minimum impact angle of 15° and the highest abrasion rates occurred at the maximum impact angle of 75°. This observation is consistent with the findings in [98]. As introduced in Section 2.2 [34, 37], concrete abrasion damage is attributed to two types of abrasion mechanisms, namely the cutting wear and impact deformation, which are closely related to the impact angle of the flow [8]. According to findings in [98], the mass loss rate increases with the impact angle ranging from 0° to 90°, however, the dominant driver of concrete abrasion damage varies significantly. This means that when the impact angle of the flow is larger than 45°, the impact deformation contributes more to the abrasion damage. On the contrary, when the impact angle is less than 45°, the cutting wear dominates the abrasion material loss [99]. Besides, it is interesting to note from Fig. 8 that the maximum
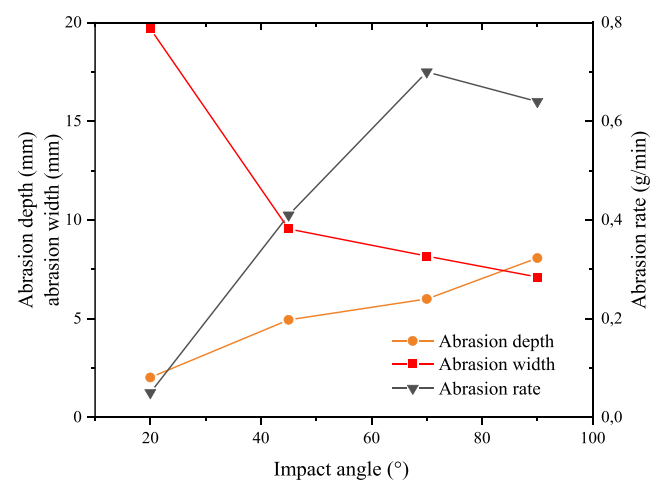
abrasion rate occurs at the medium impact angle of 70° rather than the maximum impact angle of 90° [48]. Neither the depth nor the width of abrasion is at its maximum at the impact angle of 70°. With the impact angle decreasing, the direct abrasion area increases but the abrasion depth tends to decrease. As a result, the rather "contradictory" results in Fig. 8 may be due to the different performance indicators used for quantifying concrete abrasion damage, as mentioned in Section 2.4.

5.1.5. Abrasive sediment particle properties

The properties of abrasive sediment particles can also affect concrete abrasion. Bajracharya et al. [100] found that the abrasion rates increased as the abrasive particle size increased. However, it should be noted that below a critical size of the sediment particle, the size effect may be negligible [101]. There also exists an upper limit, i.e., not necessarily the largest particle size, beyond which the abrasion rates become almost independent of any further increase in size [36]. This is due to the fact that a change of transport mode of sediments from suspension to rolling may occur and thus the velocity cannot reach the threshold for particle motion, finally resulting in a significant reduction in abrasion rates [102]. The size effect was also reported by Turowski et al. [103] who found that more than 40% of the kinetic energy was used to deliver the largest grains with a dimension of over 86 mm. These large-size particles contributed a lot to abrading concrete surfaces, whereas particles with this size class only accounted for less than 10% of the total sediment volume.

In addition, the shape of sediment particles is another important particle property concerning concrete abrasion. The local stress at the impact spot appears when abrasive sands impact or slide over the concrete surface and it increases with decreasing contact area according to the Hertzian pressure [104]. As a result, angular gravel particles would result in the production of an indentation or micro-cracks in the concrete surface, especially when the hardness of the concrete is smaller than that of abrasive particles [105]. As a typical abrasive material, the hardness of quartz sands is 7–10 Mohs whereas the hardness of normal concrete is 6–7 Mohs. Sklar and Dietrich [106] revealed that the use of quartzite sands as abrasive materials increased the abrasion rates, compared with the limestone abrasives. Bovet [107] reported that angular particles caused higher specific abrasion rates than rounded particles. However, the angularity of abrasive particles will reduce and the shape of abrasive sands tends to become round and smooth with exposure time increasing [96].

5.2. Concrete properties

5.2.1. Strength and hardness

Concrete strengths are among the most relevant factors that influence the abrasion resistance of concrete. As discussed earlier, impact deformation is one of the dominant abrasion mechanisms while the generated compression loads at the impact point can squeeze and force materials downward. The produced horizontal tensile stresses can tear the concrete surface apart [54]. In this regard, these tensile stresses are the prime culprits for crack initiation in the hardened mortar and fractures around aggregate particles. The accumulated cracks finally cause concrete abrasion damage. Many researchers explored the effects of concrete tensile strengths on abrasion damage [19,48,49,108,109,110]. Besides, the flexural strengths equal to or slightly larger than the failure stress in tension are also attractive to describe the effects of concrete strengths on abrasion resistance [20,40,94,111–113]. Compressive strengths are usually used as a parameter to assess the concrete abrasion resistance [20,40,68,114–121], although it is well acknowledged that the abrasion damage is not directly associated with the failure under compression. However, it should be noted that compressive strengths are highly associated with other properties, e.g., tensile and flexural strengths.

The available data for the effects of concrete strengths on abrasion mass loss are summarized in Fig. 9, in which it can be found that concrete abrasion damage generally decreases with the increase in concrete strength. This is because mortar phases in concrete with a low strength generally have a high porosity and low hardness, which tend to be easily abraded away under repeated hydraulic loads [122]. Moreover, according to the abrasion process theory discussed in 2.3.1, small-size aggregates in the concrete tend to be taken out totally due to the weak interfacial bond between the mortar matrix and aggregates in the low-strength concrete. From Fig. 9, it is found that the abrasion mass loss of concrete is distributed in a wide range from 0.66 g to 211.37 g. Mostly, the abrasion mass loss is smaller than 48 g, 77 g, and 129 g,

when the tensile, flexural, and compressive strengths are larger than 2 MPa, 4 MPa, and 30 MPa, respectively. As for those concrete mixtures with super-high strengths (≥120 MPa for compressive strength) [117, 123], the abrasion mass loss is approximately 0. Fig. 10 summarizes the relation between abrasion depth and concrete compressive strength [15, 55,65,68,78,85,90,115,120,124–132]. Concrete abrasion depths generally decrease with the increase of compressive strength. However, there is no significant change in the abrasion depth of concrete with super-high compressive strength (over 110 MPa). Besides, it is found that around 80% of concrete mixtures exhibit abrasion depth less than 4 mm [64,67,85,111,124,128].

As a typical material property for evaluating concrete performance and because of the easiness of measurement, concrete strengths have been frequently used as a performance indicator to consider concrete
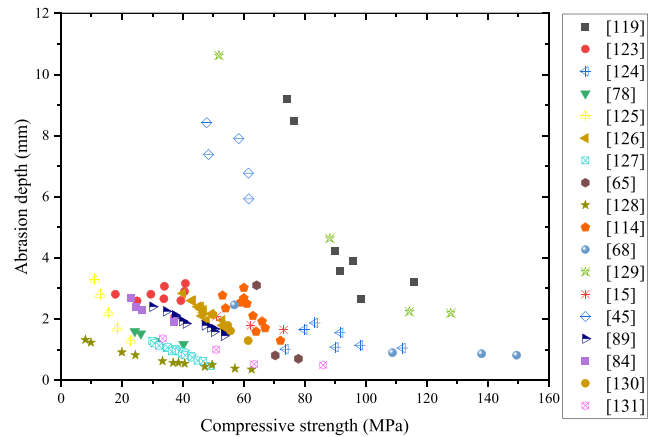
Fig. 10. Effects of concrete compressive strengths on concrete abrasion depth [15,55,65,68,78,85,90,115,120,124–132].
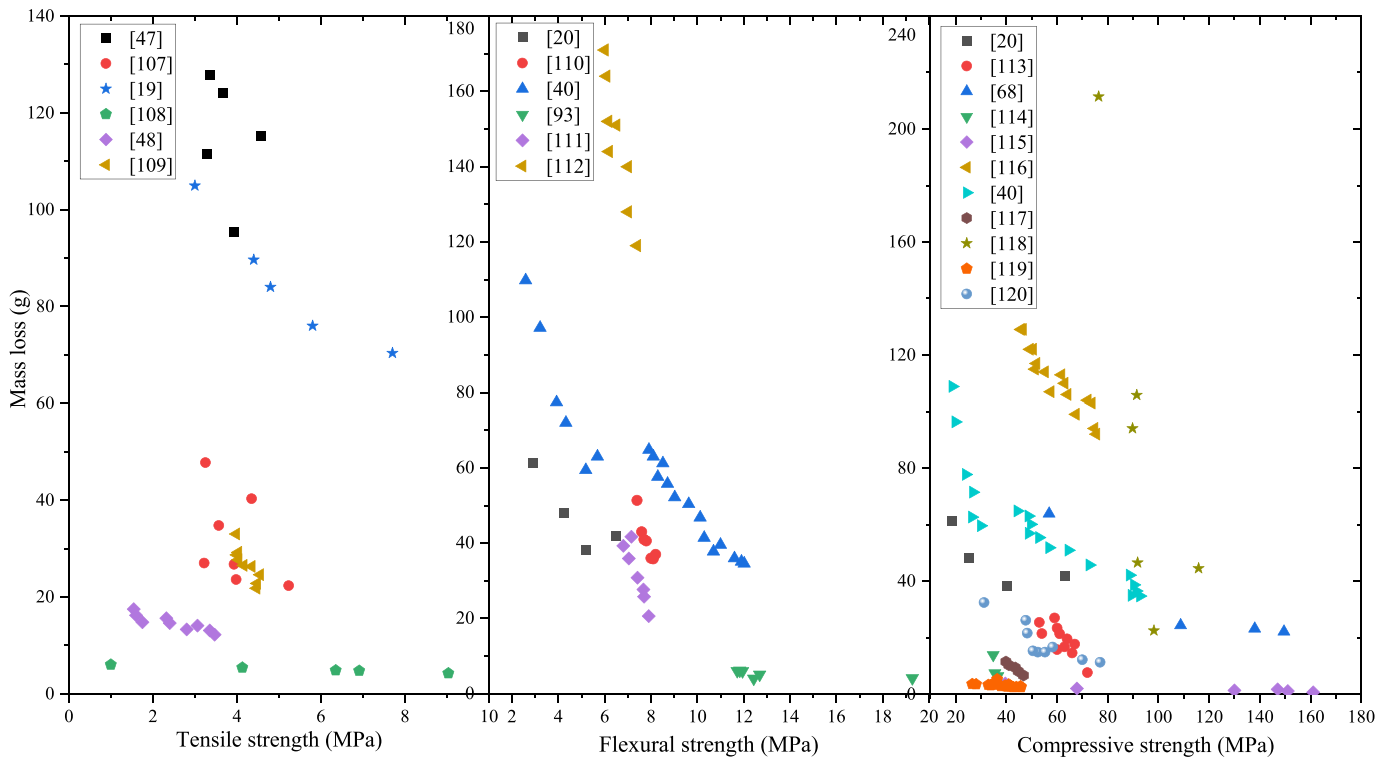
Fig. 9. Effects of concrete strengths on abrasion mass loss: tensile strengths [19,48,49,108,109,110]; flexural strengths [20,40,94,111–113]; and compressive strengths [20,40,68,114–121].

abrasion resistance. However, the applicability of the strength as a single indicator may remain questionable since the wide variation in concrete performance and flow characteristics makes it inaccurate that a single set of parameters can describe adequately the dependence of abrasion damage on strengths [133]. As a result, the governing concrete properties, e.g., porosity, and concrete hardness should be considered in the assessment of abrasion damage instead of a single parameter.

In addition, concrete hardness which is highly associated with concrete strength performance also affects the performance of the materials against abrasion penetration and plastic deformation. When the sediment-laden flow impacts the concrete with high hardness, the flow may rebound all around rather than penetrate along the micro cracks. Therefore, concrete abrasion resistance increases with the improvement in the hardness. However, after a certain point, an increase in hardness leads to reduced elasticity, and hence causes a reduction in concrete abrasion resistance [8]. As reported in [134], aggregates were major components affecting concrete hardness. The abrasion depth of concrete composed of different types of coarse aggregates (gabbro, basalt, granite, limestone, quartzite, dolomitic limestone, and trap rock) was investigated in [4,131], and results indicated that concrete with hard aggregates, e.g., granite and trap rock, experienced the least abrasion depth of less than 0.2 mm whereas concrete with limestone experienced the most loss of over 1.2 mm.

5.2.2. Toughness

Apart from concrete strength and hardness, concrete toughness is another significant parameter that affects concrete abrasion resistance from the perspective of macroscopic mechanical properties [135]. However, it has to be pointed out concrete toughness is highly associated with the tensile or flexural strengths of concrete. As a result, concrete toughness is not a focus among the existing studies on the abrasion resistance of concrete. It was reported that concrete abrasion material loss was decreased by up to 50% when the flexural toughness of concrete increased from 0.58 J to 1.01 J due to the addition of elongated rubber particles [136]. According to the findings in [137], the abrasion length of concrete decreased by 25.0% with the toughness increasing from 3430 kJ to 8410 kJ. This is most probably because the critical cracking displacement of concrete is beyond the crack affected by abrasion damage when rubber particles in the concrete mixture yield toughness. Similarly, the incorporation of fibers can increase concrete abrasion resistance by up to 28.6% since their bridging effects can delay the propagation of micro cracks and improve the toughness of concrete [48, 96]. The incorporation of plastic aggregates can also divert the propagation of micro cracks and improve concrete toughness due to their high hardness, thereby increasing concrete abrasion resistance by 54.5% [128]. Nevertheless, concrete toughness and strength/hardness may be a contradictory pair of indexes in some cases. For example, the use of silica fume may increase the compressive strength but decrease the toughness of concrete, especially due to the early cracking of the concrete [138]. Therefore, it is necessary to achieve a balance between them when considering the abrasion resistance of concrete.

5.2.3. Pore structure

According to the abrasion process described in Section 2.3.1, mortar paste peels off first from the concrete structure, followed by the total removal of individual aggregate particles. In this regard, the pore structure that affects the mechanical properties of the mortar phase has influences on concrete abrasion resistance [139]. The general trend is that the higher the concrete porosity, the lower the strength of the mortar matrix and the more the abrasion material loss of concrete [140]. According to the observations in [64], increasing the contents of voids in concrete mixtures from 23% to 28% resulted in a reduction in compressive strengths by 52%, simultaneously causing a 154% increase in concrete abrasion depth. In addition, a linear increasing trend was reported in [141,142] when concrete porosity ranged from 10% to 30%. However, further research is needed to understand the relation between

concrete porosity and abrasion resistance to get more insights into the fundamental mechanisms behind concrete abrasion damage.

5.2.4. Aggregate properties

The aggregate properties can affect the abrasion behavior of concrete as aggregates are exposed to the flow directly once the top mortar layer is abraded away. The use of aggregates with larger hardness can increase concrete hardness correspondingly, thus leading to better mechanical responses of concrete to the impact loading of the sediment-laden flow [143]. The Mohs hardness of calcined bauxite is about 8.5, higher than that of basalt aggregates (Mohs hardness: 7.0). Thus, using calcined bauxite aggregates in concrete mixtures yielded a 3.6% reduction in abrasion mass loss [115]. Among other concrete mixtures containing dolomite (Mohs hardness: 3.5–4.0) and marble (Mohs hardness: 3.0–4.0) [144], concrete containing basalt aggregates exhibited better abrasion resistance, as demonstrated by the least abrasion mass loss at 16.2 g [125,134].

Besides, the abrasion resistance of concrete is influenced by the aggregate angularity. The presence of angular aggregates may lead to the initiation of cracks induced by the local stress at the aggregate corner, thereby increasing abrasion material loss. However, the angular aggregate can interlock with the surrounding mortar well, and thus the probability of aggregate total removal decreases. It is found from Table 4 that the abrasion mass of concrete slab comprising angular aggregates is about 10.9% higher than that of the slab with rounded aggregates, which indicates the effects of the local stress play a dominant role in abrasion material loss. In addition, it is found that the abrasion mass of concrete with flaky aggregates is 20.8% higher than that of concrete with non-flaky aggregates [18]. This may be attributed to the higher specific area of flaky aggregates exposed to the flow loading. Besides the effects of the aggregate type and shape, a few studies explored the

Table 4
Summary of effects of aggregate size, angularity, flakiness, and type on concrete abrasion mass loss.

Ref.	Aggregate type	Angularity	Flakiness	Maximum size (mm)	Mass loss (g)
[40]	Basalt	Angular	Non-flaky	5.0	96.5
	Basalt	Angular	Non-flaky	13.0	62.6
	Basalt	Angular	Non-flaky	25.0	59.4
	-	50% round +50% angular	50% flaky+50% non-flaky	20.0	48.7
	-	50% round +50% angular	50% flaky+50% non-flaky	16.0	50.5
	-	50% round +50% angular	50% flaky+50% non-flaky	12.5	53.8
	-	50% round +50% angular	50% flaky+50% non-flaky	10.0	63.4
[18]	-	Angular	50% flaky+50% non-flaky	20.0	52.4
	-	Round	50% flaky+50% non-flaky	20.0	46.7
	-	50% round +50% angular	Flaky	20.0	52.0
	-	50% round +50% angular	Non-flaky	20.0	41.2
[125]	Dolomite	Angular	Non-flaky	16.0	19.1
	Marble	Angular	Non-flaky	16.0	24.5
	Basalt	Angular	Non-flaky	16.0	16.2
[115]	Basalt	Angular	Non-flaky	7.0	24.9
	Calcined bauxite	Angular	Non-flaky	7.0	24.0

influence of the maximum aggregate size on concrete abrasion resistance [18,40]. As shown in Table 4, the mass loss of concrete comprising aggregates with a maximum size of 10 mm is 30.2% higher than that of concrete comprising aggregates with a maximum size of 20 mm [18]. A similar trend was reported in [40] that concrete abrasion mass decreased by 38.8% when the maximum size of aggregates in concrete mixtures increased from 5 mm to 25 mm. This can be explained from the perspective of the concrete abrasion process as discussed in Section 2.3.1 that large-size aggregates are harder to be abraded away since larger areas can be adhered to the surrounding mortar.

6. Strategies for enhancing concrete abrasion resistance

6.1. Fiber incorporation

The inclusion of discontinuous fibers has been the most widely adopted strategy for improving concrete abrasion resistance [20–22, 120,145]. Table 5 summarizes the used fiber materials and their effects on concrete abrasion resistance. Since the tensile strengths, length, aspect ratios, and shape are different for various types of fibers, and the adopted fiber fractions range from 0.03 vol% to 16.8 vol%, the performance of fibers in improving concrete abrasion resistance varies significantly. Regardless of the properties of fibers, a general trend can be found that concrete abrasion resistance increases with the fiber contents in concrete mixtures increasing. It is found from Table 5 that increasing the contents of steel fibers from 0.5 vol% to 1.0 vol% causes a 4.7–8.8% reduction in concrete abrasion depth [146]. A similar trend was reported in [147] that abrasion mass loss was decreased by 15.1–40.6% when the content of steel fibers increased from 0.25 vol% to 0.83 vol%. Steel fibers are effective in improving concrete abrasion resistance, mainly associated with three positive effects.

The first one is associated with the hardness properties of steel fibers. This means that the presence of steel fibers with high hardness can help concrete resist deformation induced by dynamic loads and protect the surrounding mortar from abrasion damage [41], as shown in Fig. 11. This can be evidenced by the comparison analyses in [65] concrete mixtures with steel fibers outperformed the PVC fiber reinforced concrete in terms of abrasion resistance (36.7% higher) due to the higher hardness of steel fibers.

The second effect of steel fibers in improving concrete abrasion resistance is associated with their fiber-bridging properties. As mentioned above, the impact of the sediment-laden flow will cause horizontal tensile stresses in the top layer of the concrete [54]. The fibers stretching across the crack interface can transfer the tensile stress to bridging fibers and yield toughness and residual strength [161], thus minimizing and retarding the overall cracking propagation and concrete abrasion damage. The fibers with larger tensile strength and higher aspect ratios can lead to better toughness and higher abrasion resistance of the concrete. Using two types of fibers (1: aspect ratio of 55 and tensile strength of 1500 MPa; 2: aspect ratio of 40 and tensile strength of 1200 MPa), concrete abrasion mass is reduced by 15.1–40.6% and 9.6–34.9%, respectively [147]. In addition, the shape and length of steel fibers can also affect their fiber-bridging effects and concrete abrasion resistance. As seen in Table 5, the use of medium hook-ended fibers (35 mm) can lead to up to 7.6% and 51.8% increase in tensile splitting strength as compared with short straight (13 mm) and long corrugated fibers (38 mm). As expected, the largest reduction in abrasion rates (about 26%) is obtained in concrete with medium hook-ended fibers, owing to the anchorage effect of the hook-ended shape. On the contrary, the reduction in abrasion rates of concrete with long corrugated fibers (38 mm) is smallest at 9%. This is because long corrugated fibers cannot homogenously distribute in the concrete system, thus leading to a 7.4% reduction in tensile strength as compared with concrete containing medium hook-ended fibers [96]. The positive effects induced by the fiber-bridging role of steel fibers can further confirm the previous discussion in Section 5.2.2 that an increase in fracture toughness can lead to

improvement in concrete abrasion resistance.

The third effect of steel fibers can be explained by the formation of a shadow zone behind fibers, especially in the case of shallow impact angles [69], as shown in Fig. 11. Once steel fibers are exposed to the flow, the shadow region will be formed due to the highly erosion-resistant properties of fibers which protect the concrete structure behind the fibers from being abrasion loads.

It was reported in [69] that the typical values for height and length of the observed 'shadow region' were about 2–5 mm and 5–10 mm, thus leading to a decrease in abrasion area of about 10–50 mm^2 [69]. Apart from the positive effects of fiber incorporation into concrete mixtures, it should be noted excessive fibers cause physical difficulties in ensuring the considerably homogeneous distribution of the fibers within the concrete system and alter the internal pore structure of concrete. The porous interphase region between fibers and mortar matrix may accelerate the crack propagation in concrete mixtures, thus causing negative effects on concrete abrasion resistance [149]. As reported in [148], fiber volume fractions beyond 2.5 vol% may result in a significant reduction in the compressive strengths, thereby weakening the abrasion resistance of concrete.

In addition, other types of fibers, e.g., carbon fibers, basalt fibers, polyester fibers, polyvinyl alcohol (PVA) fibers, polypropylene (PP) fibers, polyacrylonitrile (PAN) fibers, polyvinyl chloride (PVC) fibers, glass fibers, and rubber fibers may also be used to enhance the concrete abrasion resistance [49,67,120,127,150,152,154,155]. Similar to steel fibers, these fibers can also act as crack arresters in concrete mixtures through their fiber-bridging effects [150]. As reported in [152], the use of longer basalt fibers (24 mm in length) caused a larger increase in concrete abrasion resistance, but the maximum abrasion resistance was obtained when fiber contents were 0.07 vol% rather than 0.14 vol%. This can be explained by the longer fibers being better at bridging cracks [152], whereas a higher amount of fibers might deteriorate their dispersion in concrete composites, which in turn might cause a decrease in strengths and abrasion resistance. The inclusion of some polymeric fibers, e.g., PVA and PAN fibers, can increase concrete abrasion resistance. This is due to the presence of hydroxyl groups in the molecular chains of PVA and PAN fibers which is beneficial for generating a strong bond with the matrix and preventing the further development and extension of cracks [162]. Besides, PAN fibers with an uneven groove shape can be interlocked closely with the surrounding mortar matrix, therefore forming a disordered "skeleton" structure. The "skeleton" structure can ensure the continuity of the internal structure of the concrete and prevent the generation of microcracks [153]. According to the findings in [163], less peeling damage of mortar is observed and a 7.0–17.5% increase in abrasion resistance can be investigated when using 0.1–0.4 vol% PAN fibers. This is because the presence of PAN fibers with kidney shape cross-section can enable 91% larger flexural strength.

However, the application of PVA and PAN fibers in concrete mixtures is restrained due to their exceptionally high costs and environmental impacts in the production and manufacturing process [164]. In this case, waste and recycled fibrous materials, e.g., PP fibers, rubber fibers, glass fibers, and PVC fibers have become an alternative solution in the construction industries [154,165,166], which can not only improve concrete abrasion resistance but also contribute a lot to the reduction of solid wastes (waste tire, polymer, glass, and PVC cables). The enhancement effects of PP fibers for concrete abrasion resistance are highly associated with their tensile strength. As reported in [21,49], using PP fibers with larger tensile strength (560–770 MPa) can lead to 37.4% reduction in abrasion mass loss, while the abrasion mass loss can only be reduced by 7.1% by incorporating PP fibers with tensile strength of about 300 MPa. Abrasion depth of concrete with rubber fibers is decreased by 7.3–17.6% due to their brush effects of rubber fibers [156].

In addition to industrial fibers, natural fibers can also be used in concrete mixtures [120,158]. As reported in [158], the abrasion resistance of concrete containing 0.97 vol% pig fibers can be increased by

Table 5
Summary of the effects of fiber incorporation on concrete abrasion resistance.

Ref.	Type of fiber	Tensile strength of fiber (MPa)	Length (mm)	Diameter (mm)	Aspect ratio	Fiber shape	Content (vol%)	28-d compressive strength (MPa)	Tensile strength (MPa)	Outcome
[148]	Steel fiber	1100	5	-	30	Straight	2.00	55.2	-	42.0% reduction in abrasion weight loss
[147]							0.25	72.1	3.3	9.6% reduction in abrasion mass loss
	Steel fiber	1200	30	0.75	40	Hook-ended	0.45	59.9	3.7	16.0% reduction in abrasion mass loss
							0.64	58.2	4.4	24.5% reduction in abrasion mass loss
							0.83	55.0	4.9	34.9% reduction in abrasion mass loss
	Steel fiber	1500	30	0.55	55	Hook-ended	0.25	69.5	3.4	15.1% reduction in abrasion mass loss
							0.45	64.5	3.8	20.8% reduction in abrasion mass loss
							0.64	59.7	4.4	28.3% reduction in abrasion mass loss
							0.83	57.4	5.0	40.6% reduction in abrasion mass loss
[146]	Steel fiber	2600	15	0.200	75	Straight	0.50	28.7	3.8	4.7% reduction in abrasion depth
							0.75	34.4	4.5	7.9% reduction in abrasion depth
							1.00	35.3	4.7	8.8% reduction in abrasion depth
[96]	Steel fiber	2850	13	0.200		Straight	1.00	86.7	7.4	12.5% reduction in abrasion rates
		1120	35	0.550		Hook-ended	1.00	80.5	7.9	26.0% reduction in abrasion rates
		650	38	2.100		Corrugated	1.00	75.9	7.3	9.0% reduction in abrasion rates
		1120	35	0.550		Hook-ended	0.50	63.4	6.0	8.3% reduction in abrasion rates
		1120	35	0.550		Hook-ended	1.50	102.6	9.6	28.4% reduction in abrasion rates
[20]	Steel fiber	1400	30	0.500	60	Hook-ended	0.90	91.8	-	17.0% reduction in mass loss and 11% reduction in abrasion depth
	PP fiber	310	19	1.000	50	Straight	0.20	98.2	-	25.8% reduction in mass loss and 16.4% reduction in abrasion depth
[149]	Steel fiber	1050	30	0.750	-	Hook-ended	1.00	51.0	-	8.0% reduction in abrasion loss
[65]	Steel fiber	-	50	-	-	Straight	0.90	91.8	-	30.0% reduction in mass loss
	PVC fiber	-	19	-	-	Straight	0.13	98.3	-	19.0% reduction in mass loss
[150]	Carbon fiber	690	5	0.010	-	Straight	0.27	-	-	40.0% reduction in wear depth
[151]	Carbon fiber	4100	2	0.070	-	Straight	5.60	48.1	2.8	16.3% reduction in weight loss
							11.20	53.5	3.5	25.6% reduction in weight loss
							16.80	51.6	3.2	14.0% reduction in weight loss
[152]	Basalt fiber	-	12	0.013–0.020	-	Straight	0.07	62.4	-	1.8% reduction in abrasion volume loss
			12				0.14	56.9	-	4.4% reduction in abrasion volume loss
			24				0.07	63.5	-	4.0% reduction in abrasion volume loss
			24				0.14	58.9	-	3.8% reduction in abrasion volume loss
[67]	Polyester fiber	400–600	12	0.030–0.050	-	Straight	0.03	32.8	-	3.1% reduction in abrasion depth
							0.04	33.5	-	6.3% reduction in abrasion depth

(continued on next page)

Table 5 (*continued*)

Ref.	Type of fiber	Tensile strength of fiber (MPa)	Length (mm)	Diameter (mm)	Aspect ratio	Fiber shape	Content (vol%)	28-d compressive strength (MPa)	Tensile strength (MPa)	Outcome
[48]	Polyester fiber	-	-	-	-	Straight	0.05	33.5	-	9.4% reduction in abrasion depth
							0.20	37.4	3.3	12.7% reduction in abrasion rates
							0.40	38.1	3.7	2.8% reduction in abrasion rates
							0.60	34.8	3.9	25.4% reduction in abrasion rates
[68]	PE fiber	2500	6, 12, 18	0.027	-	Straight	0.04	45.1	-	11.3% reduction in mass loss
							0.08	45.9	-	21.4% reduction in mass loss
							0.12	46.5	-	31.2% reduction in mass loss
	PVA fiber	1830	12	0.015			0.09	46.5	-	9.1% reduction in mass loss
	PAN fiber	800	12	0.013			0.08	44.5	-	16.8% reduction in mass loss
	Basalt fiber	2300	12	0.017			0.17	48.7	-	4.3% reduction in mass loss
[127]	PVA fiber	1660	12 ± 1	0.080–0.090	-	Straight	0.10	45.3	3.1	9.3% improvement in abrasion resistance strength[a]
[49]	PP fiber	274.0 ± 26.9	12	-	-	Straight	0.10	38.0	3.5	13.5% reduction in abrasion mass loss
	PP fiber	300.7 ± 31.7	12	-	-	Straight	0.10	30.7	2.8	7.1% reduction in abrasion mass loss
[22]	PP fiber	400	20	0.450	-	Straight	0.25	43.4	4.4	2.4% reduction in abrasion volume loss
							0.50	40.8	4.7	4.7% reduction in abrasion volume loss
							0.75	39.2	4.8	9.7% reduction in abrasion volume loss
							1.00	38.5	4.5	13.6% reduction in abrasion volume loss
							1.25	36.3	4.3	11.0% reduction in abrasion volume loss
[21]	PP fiber	560–770	12–19	0.100	-	Straight	0.05	52.1	-	23.0% reduction in mass loss
							0.10	53.6	-	37.4% reduction in mass loss
							0.15	46.8	-	32.5% increase in mass loss
[153]	PAN fiber	1051	12	0.012	-	Uneven groove	0.10	77.3	3.7	7.0% reduction in abrasion mass loss per unit area
							0.20	76.8	3.7	12.4% reduction in abrasion mass loss per unit area
							0.30	75.7	3.9	15.0% reduction in abrasion mass loss per unit area
							0.40	76.1	3.8	17.5% reduction in abrasion mass loss per unit area
[154]	Glass fiber	1750	10	0.012	852	Straight	1.00	40.7	-	7.1% reduction in weight loss
							1.50	38.2	-	24.9% reduction in weight loss
							2.00	36.1	-	29.4% reduction in weight loss
[155]	Rubber fiber	-	20	2.000–5.000	4–10	Straight	1.39	39.4	-	5.1% reduction in abrasion depth
							2.78	36.1	-	14.5% reduction in abrasion depth
							4.17	30.9	-	17.9% reduction in abrasion depth
							5.56	27.2	-	23.9% reduction in abrasion depth

(*continued on next page*)

Table 5 (*continued*)

Ref.	Type of fiber	Tensile strength of fiber (MPa)	Length (mm)	Diameter (mm)	Aspect ratio	Fiber shape	Content (vol%)	28-d compressive strength (MPa)	Tensile strength (MPa)	Outcome
[156]	Rubber fiber	-	20	2.000–5.000	-	Straight	6.95	23.8	-	38.5% reduction in abrasion depth
							5.00	36.9	-	7.3% reduction in abrasion depth
							10.00	34.0	-	13.1% reduction in abrasion depth
							15.00	30.9	-	17.6% reduction in abrasion depth
[157]	Hybrid fiber (steel fiber, glass fiber, synthetic fiber, PP fiber)	1150, 3400, 338 and 620	30, 10, 40, and 40	0.900, 0.013, 0.750, and 0.750	33.33, 769, 53.33, and 53.33	Straight	1.00	36.4	-	16.7% increment in abrasion mass loss
[158]	Natural fiber (pig hair)	99	36	0.160	249	Straight	0.97	72.2	-	28.8% reduction in mass loss
							1.94	71.8	-	20.3% reduction in mass loss
							2.91	68.4	-	10.7% reduction in mass loss
[120]	Natural fiber (coir fiber)	-	20–50	-	170–200	Straight	0.11	44.0	-	6.0–9.0% reduction in mass loss rates
							0.22	45.7	-	15.0–17.0% reduction in the mass loss rates
							0.33	39.5	-	21.0–27.0% reduction in the mass loss rates
[159]	Natural fiber (coir fiber)	-	-	-	-	Straight	0.30	11.4	3.5	8.9% reduction in abrasion depth
							0.40	7.9	2.3	30.0% increase in abrasion depth
							0.50	6.9	2.0	60.0% increase in abrasion depth

[a] The abrasion resistance strength is calculated by multiplying the abrasion time and the abraded surface area which is then divided by the abrasion mass loss.

28.8%, larger than that of concrete containing 1.94 vol% and 2.91 vol% pig fibers. This may be explained by the fact that the appropriate content of pig fibers with large water absorption capacity can reduce the effective water-cement ratio, thus lowering the porosity in hardened concrete and improving the abrasion resistance. However, when large contents of pig fibers with low density are incorporated and float up in the top surface layer, mortar paste would be more easily damaged [167]. As reported in [120,159], there was a limit for coir fiber content (0.3 vol%) over which, the abrasion depth was increased by up to 60%. This may be due to the fact that the natural fibers with tensile strength of less than 100 MPa are insufficient in fiber bridging effects [168]. However, the addition of coir fibers with a length of 20–50 mm leads to a decrease in concrete workability, thus resulting in an increase in the concrete porosity and abrasion damage.

In summary, it is found that fiber incorporation can lead to an almost consistent tendency in concrete abrasion resistance. However, previous studies mainly focused on the fiber types and contents of the abrasion resistance of concrete. Further studies, e.g., concerning the effects of fiber embedment angle in concrete and interfacial bond with mortar are far from being sufficient.

6.2. Use of supplementary cementitious materials (SCMs)

SCMs play a significant role in mitigating carbon dioxide emissions associated with concrete production. Besides, the use of SCMs can improve the long-term mechanical properties and durability of concrete mixtures [169]. SCMs are frequently used in concrete mixtures due to either pozzolanic or hydraulic activity, which is closely associated with their chemical compositions. The chemistry and hydrate phases of several types of commonly used SCMs, e.g., fly ash, silica fume, and ground granulated blast-furnace slag (GGBS) are shown in Fig. 12 [170]. It should be noticed that the C–S–H phase accounts for the major part of

the hydrate phases, which is the most important phase in hydrated cement systems. It has been qualitatively observed that the incorporation of fly ash and silica fume results in the reduction of the amount of portlandite but leads to the increment in the formation of C–S–H gels. As for GGBS, little effects could be identified on the amount of portlandite in the hydrate phases when compared with that of pure cement systems, unless the substitution ratio is high [170]. The effects of SCM types and contents on concrete abrasion depths and mass loss are summarized in Tables 6 and 7. The adopted contents of fly ash and GGBS are in a wide range of 15–70 wt% and 10–60 wt% while the contents of silica fume are smaller ranging from 5 wt% to 20 wt%. Besides, the effects of some novel cementitious materials, e.g., Nano-TiO$_2$, Nano-SiO$_2$, Cathode ray tube (CRT) glass powders, and rice husk ash are also investigated. Nevertheless, it is found that using SCMs in concrete mixtures does not lead to a consistent tendency in concrete abrasion resistance.

6.2.1. Fly ash

Fly ash has been one of the most commonly used SCMs in the construction of abrasion-resistant concrete structures [55,81,82,84,171, 179]. As seen in Table 5, the effects of fly ash as a replacement for cement on concrete abrasion resistance are inconsistent. With class F fly ash contents of no more than 22.5 wt%, concrete abrasion depth can be reduced by up to 18.4% [66,84]. This is because the use of fly ash can result in the formation of a less porous and denser microstructure system through its both physical and chemical effects during the freshly mixed and subsequent hydrating states [180]. Besides, the addition of fly ash can improve the interfacial bond of the aggregate-mortar matrix [180], which implies the role of fly ash in mitigating crack development. The interface behavior and pore structure as well as strength of concrete can affect concrete abrasion resistance which is consistent with the previous discussion in Sections 5.2.1 and 5.2.3. However, increasing fly ash contents to 30.0 wt% and 37.5 wt% would weaken concrete
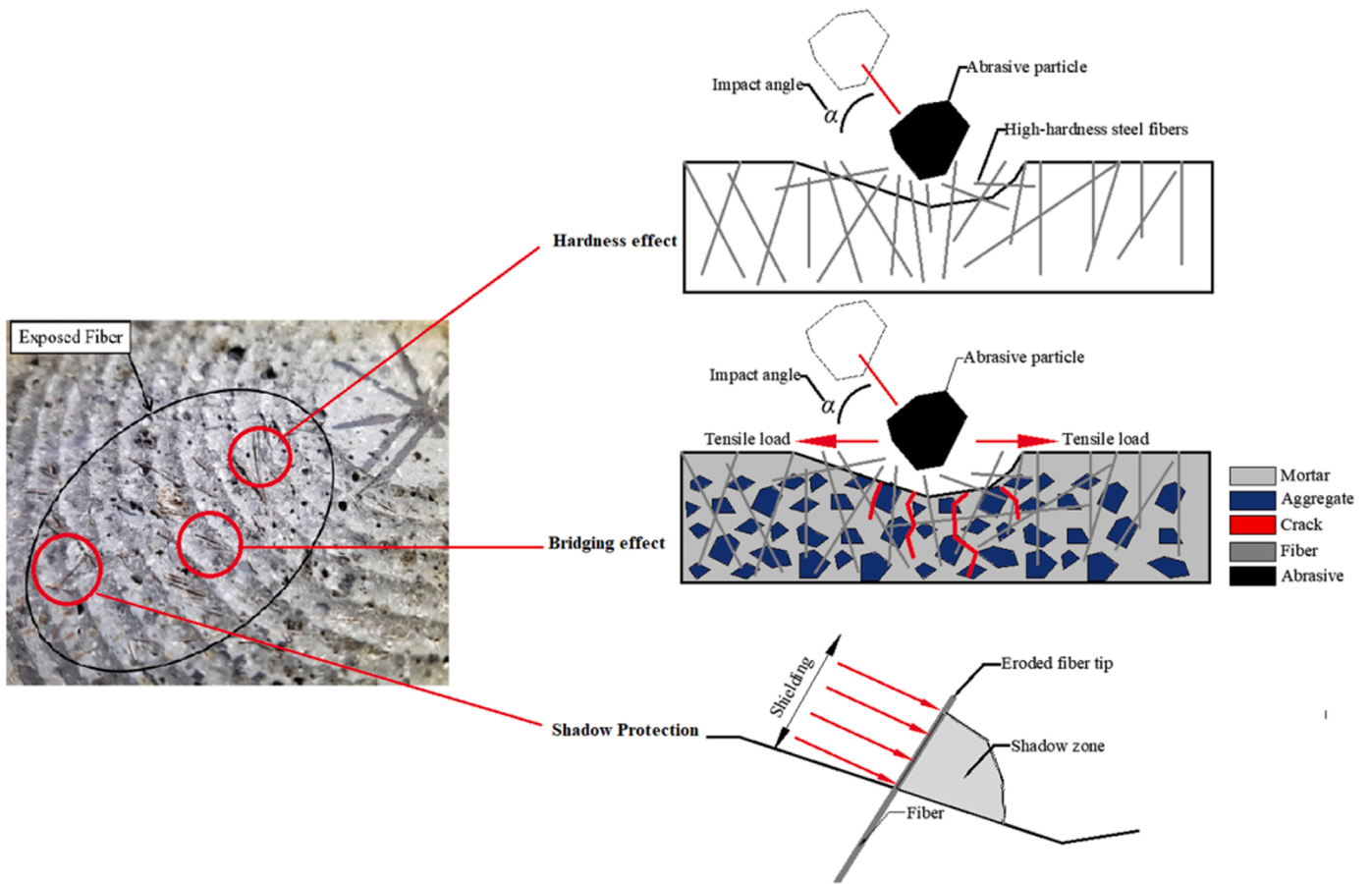
Fig. 11. Strengthening effects of steel fibers on concrete abrasion resistance [41,69,160].
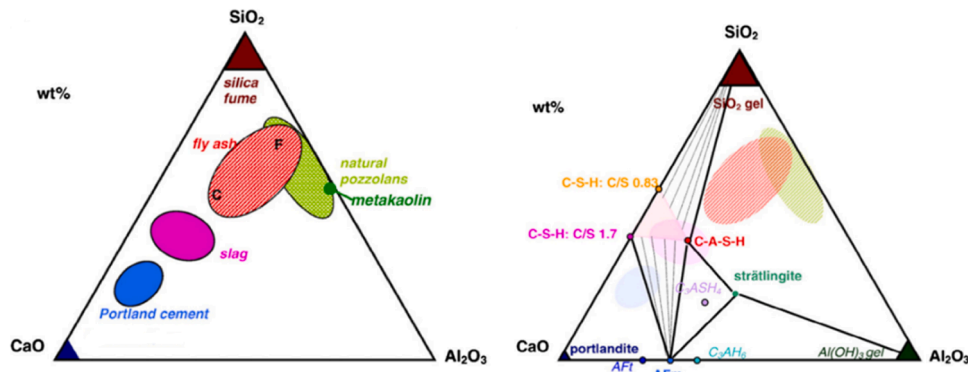

Fig. 12. Main chemistry diagram of fly ash, silica fume, and GGBS, and the hydrate phases in the CaO–Al_2O_3–SiO_2 system [170].

compressive strength by 11.9–15.3%, and thus concrete abrasion resistance is reduced by 6.3–15.5% [84]. As is known, the CaO content of fly ash is lower as compared with Portland cement, especially for class F fly ash with CaO contents less than 18% [181]. The loss of the amount of CaO contents leads to a reduction in the generation of C-S-H gels, thereby inhibiting the development of concrete strength and abrasion resistance [182]. As reported in [81,138], concrete compressive strengths were decreased by 28.2–37.9% and abrasion depths were increased by 44.8–100.0% due to the loss of hydration reaction products at a higher replacement level of class F fly ash (40–50 wt%).

Unlike class F fly ash, the CaO contents of class C fly ash are generally larger than 18.0 wt%. High-calcium fly ash can promote hydration reactions, thus producing more calcium silicate hydrate (C-S-H) and

calcium aluminate hydrate (C–A–H). The produced hydration products can improve the pore structure of concrete, which is highly related to concrete abrasion resistance (as discussed in Section 5.2.3). As reported in [183], concrete containing class C fly ash possessed superior abrasion resistance as compared with concrete containing class F fly ash. Replacing cement with 18.0 wt% fly ash can lead to a 9.5% decrease in concrete abrasion depth as compared with concrete with 36.0 wt% fly ash (2.3%) [78]. This is because higher contents of fly ash may lead to a reduction in C-S-H gels and thereby weaken concrete compressive strength (see Table 5). Moreover, negative effects induced by high-volume fly ash were reported in [82] that concrete containing 50.0 wt% and 70.0 wt% class C fly ash exhibited 42.0% and 77.5% rise in abrasion depths (2.84 mm and 3.55 mm), as compared with concrete

Table 6
Summary of effects of contents and types of SCMs on concrete abrasion depth.

Ref.	Additive type	Content (wt%)	W/B ratio	28-d compressive strength (MPa)	Abrasion depth (mm)	Effects on abrasion depth
[84]	Class F fly ash	0.0	0.40	61.5	1.74	0.0%
		15.0	0.40	60.4	1.42	-18.4%
		22.5	0.40	55.9	1.57	-9.8%
		30.0	0.40	54.2	1.85	+6.3%
		37.5	0.40	52.1	2.01	+15.5%
[81]	Class F fly ash	0.0	0.41	37.2	0.58	0.0%
		40.0	0.40	26.7	0.84	+44.8%
		45.0	0.41	24.7	1.02	+75.9%
		50.0	0.40	23.1	1.16	+100%
[171]	Class F fly ash	0.0	0.35	58.2	1.23	0.0%
		15.0	0.35	55.6	1.42	+15.8%
		25.0	0.35	53.8	1.49	+20.8%
		35.0	0.35	45.2	1.49	+20.8%
[82]	Class C fly ash	0.0	0.36	43.4	2.00	0.0%
		50.0	0.33	31.9	2.84	+42.0%
		70.0	0.36	17.5	3.55	+77.5%
[78]	Class C fly ash	0.0	0.35	43.1	2.10	0.0%
		18	0.35	48.0	1.90	-9.5%
		36	0.35	47.1	2.05	-2.3%
[57]	Fluidal fly ash	0.0	0.40	48.4	7.39	0.0%
		20.0	0.40	61.5	6.75	-8.6%
		30.0	0.40	61.6	5.94	-19.6%
		40.0	0.40	58.3	7.91	+7.0%
		50.0	0.40	47.8	8.43	+22.7%
[172]	GGBS	0.0	0.52	35.2	32.20	0.0%
		20.0	0.55	35.9	30.10	-6.5%
		40.0	0.54	38.3	20.90	-35.1%
		60.0	0.58	32.9	50.30	+56.2%
[124]	Silica fume	0.0	0.40	47.0	1.33	0.0%
		10.0	0.40	22.0	1.30	-2.3%
		20.0	0.40	30.7	1.21	-9.0%
[173]	Nano-TiO$_2$	0.0	0.42	59.1	26.57	0.0%
		1.0	0.42	69.7	9.47	-64.4%
		3.0	0.42	66.6	10.71	-59.7%
		5.0	0.42	60.0	13.93	-47.6%
	Nano-SiO$_2$	1.0	0.42	66.4	10.33	-16.2%
		3.0	0.42	61.2	13.23	-50.2%
[174]	CRT glass powders	0	0.44	54.7	1.49	0.0%
		5.0	0.44	49.8	1.49	0.0%
		10.0	0.44	45.3	1.46	-2.0%
		15.0	0.44	56.3	1.47	-1.3%
		20.0	0.44	46.5	1.49	0.0%
		35.0	0.44	34.8	1.60	+7.4%
[175]	Rice husk ash	0	0.47	32.8	0.72	0.0%
		5	0.47	34.0	0.62	-13.9%
		10	0.47	35.8	0.59	-18.1%
		15	0.47	35.1	0.63	-12.5%
		20	0.47	33.1	0.68	-5.6%

without fly ash (2.00 mm) [82]. This is consistent with the trend of concrete containing high-volume class F fly ash. Besides, the curing age can affect the abrasion resistance of fly ash concrete, as reported in [125].

In summary, using fly ash as the replacement for cement may not always lead to the improvement of concrete abrasion resistance. The moderate levels of cement replaced by fly ash may cause positive effects on concrete abrasion resistance while replacing a larger part of the cement is not recommended as far as concrete strength and abrasion resistance is concerned. Besides, the abrasion resistance of concrete incorporating fly ash is largely determined by the chemical properties of fly ash. Consequently, it should be noted that both the fly ash types and the appropriate contents of fly ash that can have positive influences on concrete abrasion resistance are largely subject to debate [98]. More studies are required to understand the effects of fly ash contents and types on the interface behavior, pore structure, and strength to get more insights into concrete abrasion resistance.

6.2.2. Silica fume

As seen in Tables 6 and 7, a general trend can be found that incorporating silica fume (0.0–20.0 wt%) in concrete mixtures can

considerably decrease concrete abrasion depth and concrete mass loss by up to 9.0% and 30.1%. Due to the small particle sizes (typically between 0.1–0.3 μm), silica fume may be used for filling the micro voids in the mortar phase and strengthening the interfacial zones between coarse aggregates and mortar [184]. More importantly, silica fume has high contents of SiO$_2$ in a range of between 85 wt% and 98 wt%. Together with the high surface area (small particle sizes), silica fume can react effectively with portlandite from cement hydration and generate secondary C-S-H gels. Thus, an optimized microstructure can be formed, thereby increasing concrete strengths and strengthening concrete abrasion resistance [134]. As reported in [17], with the contents of silica fume increasing from 0 wt% to 10.0 wt%, concrete strength increased by 23.0% and abrasion mass loss decreased by 25.4%. However, adding silica fume to concrete mixtures may bring negative effects, such as decreasing concrete toughness and increasing the risk of early cracking of the concrete [113]. Therefore, the amount of silica fume to be used for replacing cement should be considered with caution as excessive silica fume may lead to cracking, especially when the curing conditions are improper, e.g., high-temperature curing [131]. This is consistent with the findings in [98] where an upper limit value was proposed (not exceeding 20.0 wt%) for using silica fume as a replacement for cement,

Table 7

Summary of effects of contents and types of SCMs on concrete abrasion mass loss.

Ref.	Type	Content (wt%)	W/B ratio	28-d compressive strength (MPa)	Abrasion mass loss (g)	Effects on abrasion mass loss
[176]	GGBS	0.0	0.48	34.9	11.60	0.0%
		20.0	0.48	35.5	8.40	-27.6%
		40.0	0.48	36.7	5.60	-51.7%
		60.0	0.48	39.2	21.10	+81.9%
		0.0	0.55	36.0	6.96	0.0%
		20.0	0.55	44.0	5.53	-20.5%
		40.0	0.55	45.0	4.08	-41.4%
		0.0	0.55	30.0	9.80	0.0%
		20.0	0.55	30.0	10.51	+7.2%
[177]	GGBS	40.0	0.55	32.0	12.14	23.9%
		0.0	0.35	66.0	3.16	0.0%
		20.0	0.35	65.0	4.42	+39.9%
		40.0	0.35	70.0	6.36	+101.3%
		0.0	0.35	46.0	5.37	+69.9%
		20.0	0.35	49.0	5.68	+79.7%
		40.0	0.35	51.0	7.14	+125.9%
		0.0	0.46	-	39.31	0.0%
		10.0	0.46	-	35.93	-8.6%
		20.0	0.46	-	30.83	-21.6%
[178]	GGBS	30.0	0.46	-	27.48	-30.1%
		40.0	0.46	-	20.64	-47.5%
		50.0	0.46	-	25.99	-33.9%
		60.0	0.46	-	41.71	+6.1%
		0.0	0.36	61.4	120.60	0.0%
[17]	Silica fume	5.0	0.38	72.6	104.40	-13.4%
		10.0	0.40	75.5	90.00	-25.4%
		0.0	0.50	39.3	509.00	0.0%
[138]	Silica fume	5.0	0.50	47.3	406.00	-20.2%
		10.0	0.50	50.4	356.00	-30.1%

beyond which concrete abrasion resistance may decrease.

6.2.3. Granulated blast-furnace slag (GGBS)

GGBS can be utilized as a partial replacement for Portland cement. This is primarily due to the high calcium content of GGBS, thus endowing its hydraulic activity and potentiality for improving concrete abrasion resistance. As reported in [185], concrete containing 20.0 wt% and 40.0 wt% GGBS exhibited a marginal increase in abrasion resistance by 0.4% and 0.7%, respectively [185]. According to the findings in [176], increasing the content of GGBS from 0 wt% to 20 wt% and 40 wt% resulted in a significant decrease in concrete abrasion mass loss by 27.6% and 51.7%, while further addition of GGBS to 60 wt% caused an 81.9% increase in abrasion mass loss [176]. This is most probably because not all cementitious materials can participate in the pozzolanic reaction in the case of high contents of GGBS. Similar results reported in [109] indicated that there was a limit for GGBS content (50 wt%) over which, the thermal expansion and autogenous shrinkage may induce cracks, thus impairing the concrete strength and abrasion resistance.

Apart from fly ash, silica fume, and GGBS, nano silica [186], palm oil fuel ash [22], ferronickel slag [178], CRT glass powders [174], and rice husk ash [175] with potential pozzolanic properties, have also been incorporated in concrete mixtures aiming to improve concrete abrasion resistance. Although there is research progress in using SCMs to improve concrete abrasion resistance, more work is required to understand important aspects, e.g., the appropriate contents and the associated mechanisms. It is worth mentioning that alternative and sustainable SCMs determine the sustainable future (common SCMs have almost been used to the maximum potential), but their effects and mechanisms on concrete abrasion resistance still need systematic investigations.

6.3. Rubber particle incorporation

Some studies have investigated the effects of rubber particles on the abrasion resistance of concrete, shown in Fig. 13 where inconsistent results are reported [187–190]. However, it is found concrete abrasion resistance is generally increased by up to 76.9% with the use of rubber particles less than 10.0 wt% for partial replacement of fine aggregates.
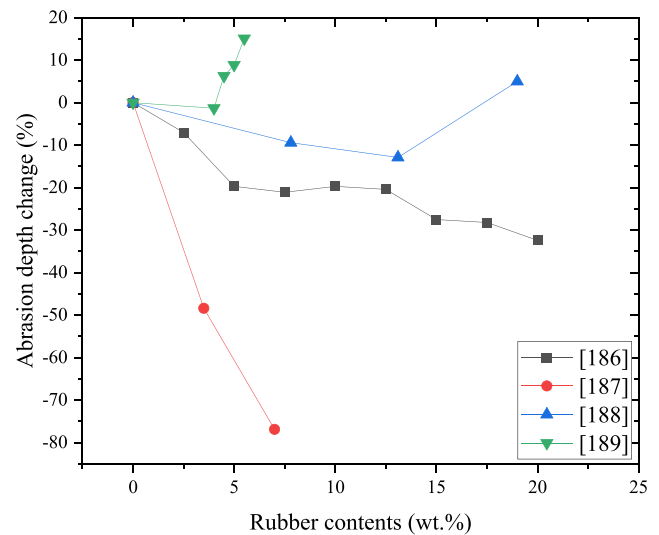

Fig. 13. The effects of rubber contents on concrete abrasion depth [187–190].

This is because the inclusion of rubber particles can absorb energy and act as brush tools as well as springs. As discussed in Section 2.2, energy conversion is involved in the concrete abrasion process, which is highly related to concrete cracking and abrasion damage evolution. Besides, the rubber particles protruding out of the abrasion surface can serve as brushes which can prevent the surface layer of the concrete from continuous sliding of abrasive particles. Moreover, according to the investigations in [191], rubber particles would act as the impedance and springs to cause a delay in crack initiation and propagation, and distributed rubber powders may prevent the catastrophic failure of concrete.

As reported in [187], concrete abrasion depth was reduced with the rubber contents increasing to 20.0 wt%. However, according to the findings in [189], negative effects occurred with increasing rubber

content up to a certain level (13.1 wt%), beyond which concrete abrasion depth increased by 5.0%. This is most probably due to the weak interface between rubber particles and mortar in high W/C concrete (0.50). The weak interface generally acts as an inner flaw leading to the crack initiation and accelerating the breakdown of the cement matrix and abrasion material loss [192]. According to the results in [190], the abrasion depth increased once the rubber contents were larger than 4.0 wt%. This may be because there is no significant change in the energy absorption capacity and spring effects when small contents of large-size rubber particles are incorporated but a significant reduction in the interfacial bond between rubber particles and mortar. Nevertheless, it has to be pointed out that fine rubber particles passing from a 1-mm sieve may be interlocked with mortar better as compared with tire chips and crumb rubber. Thus, using 7.0 wt% finer rubber particles can lead to up to 33.2% reduction in the abrasion depth of concrete [188].

Considering the hydrophobicity of rubber particles and their poor interface bond performance, it is desirable to incorporate a modest content of rubber aggregates into the concrete to avoid a significant decrease in concrete performance [193]. However, the poor interfacial bond behavior and the impact on overall concrete properties of rubber particles have not been systematically analyzed, which hinders the potential engineering applications. Therefore, further studies are required to comprehensively understand the weak interface effects and possibly explore modification and optimization techniques aiming at strengthening the interface between rubber particles and mortar, e.g., using polyvinyl alcohol (PVA) solution to treat the rubber surface and improve its hydrophilicity properties [192].

Apart from the approaches discussed above, which are means to improve the intrinsic abrasion resistance of concrete, a surface protective layer/lining has been proposed to protect the concrete beneath hydraulic structures. As reported in [194], polyurea waterproof adhesive (PUA), iron sheet (IS), and rubber layer (RB) can effectively restrain the evolution of abrasion damage, which can be evidenced by 73–79%, 80–92%, and 12–16% reduction in abrasion rates. The abrasion depth of concrete elements with surfaces coated by impregnating paints is about 5 times smaller than that without surface protective layers, indicating the effectiveness of impregnations in filling pores on the concrete surface layer and improving its abrasion resistance. As discussed in Section 5.2.1, the abrasion resistance of concrete is closely related to the compressive strength, so high-strength concrete (over 80 MPa) may be applied as a protective layer for hydraulic structures [195]. Geopolymer and flexible protective coating materials are in-situ applied on the concrete surfaces along the coast to protect concrete structures exposed to the marine environment [196]. However, it is worth mentioning that the experience from the field application is not always that encouraging with surface protective materials, which may most likely be due to, e.g., the complexity added in the field implementation, imperfect surface bonding, or the thermal incompatibility between coating materials and the concrete beneath [192]. Therefore, very limited studies have conducted abrasion tests to investigate the effects of protective materials on the abrasion resistance of hydraulic concrete structures. Further research can be concentrated on strengthening the surface bond between concrete and protective layers to promote the practical applications of surface protective materials.

7. Research gaps and future perspectives

7.1. Research gaps

Based on the discussions above, there are some major research gaps within the field of concrete abrasion studies. Some of them are listed in the following:

(1) As discussed in Section 3, standard testing methods that can effectively simulate abrasion characteristics and reflect the complex hydraulic conditions in the field are still missing. There

remains a significant gap between the results obtained from laboratories and the field.

(2) In Section 2.4, the description and characterization of concrete abrasion damage are strongly influenced by the performance indicators adopted. Apart from the frequently used material (mass/volume) loss, the affected abrasion area is of particular interest, including the abrasion depth, groove shape/profile, etc. However, reliable quantifications of these parameters are not always that straightforward, partly due to, e.g., the rather shallow depths of the abraded areas in laboratory tests. Consequently, the reported experimental results and conclusions deviate, or they are even contradictory to each other in the literature (see Section 5.1.4).

(3) As presented in Section 2.2, the abrasion damage of concrete is caused mainly by mechanical actions, including cutting abrasion and impact actions, while in field conditions concrete can also be affected by chemical and physicochemical processes, e.g., freeze-thaw [197], sulfate, and chemical attacks. In most cases, abrasion studies are conducted without considering other degradation mechanisms simultaneously. In order to reflect the field cases, studying the coupling effects of several degradation mechanisms is important, which also seems a significant research gap to be filled.

(4) Although extensive models have been established to predict concrete abrasion damage, the comparison of different models is still lacking. Besides, the application of models to complicated field conditions may be questionable.

(5) In Section 5, it can be found that there have been significant efforts to reveal the influences of important factors on concrete abrasion damage, including typical hydraulic parameters and concrete properties. However, due to the complexity of the concrete abrasion problem, quantifying the impact of each parameter is never an easy task, which is especially true when several influencing parameters are involved and sometimes intertwined in a single process. It may be adequate to state that the current understanding of the effects of the various influencing factors on concrete abrasion is generally qualitative. Further quantification analyses are still needed to understand the working mechanisms incurred by the different factors.

(6) As discussed in Section 6, various materials, including e.g., several types of fibers, SCMs, and rubber particles, have been added to concrete mixtures, and surface protective materials have also been applied to improve concrete abrasion resistance. However, the enhancing performance of additions on concrete properties and particularly the fundamental mechanisms behind them are far from being fully understood. Besides, the abrasion resistance of concrete incorporating additions is largely dependent upon their specific types and dosages. However, the research on a specific addition type is normally limited, and the appropriate contents of additions are often debatable. The research on sustainable, eco-friendly, and effective additions in concrete mixtures is of particular interest, e.g., biochar [198], ceramic waste powder [199], and rice husk ash [175], while so far relevant studies remain limited.

7.2. Future perspectives

In regards to the durability performance of concrete for hydraulic structures exposed to abrasion risks, the following aspects may be considered for future research:

(1) Standardized test methods and procedures need to be established in which a good correlation between laboratory tests and field conditions can be achieved. In this context, maybe more than one test method should be considered to account for the different working mechanisms involved in the different abrasion zones.

(2) More accurate quantification of concrete abrasion damage, e.g., the abrasion depth and the profile of the abrasion area, can be explored. Such data would be of high relevance for more in-depth analyses and correlating with numerical studies.

(3) Studies on the abrasion damage of concrete for hydraulic structures under various environmental loadings or degradation mechanisms are of high value, as they can be more representative in field conditions.

(4) Fundamental mechanisms behind the effects of various additions incorporated into concrete mixtures for the enhancement of abrasion resistance need to be further explored. In addition, more sustainable, eco-friendly, and effective additions should be considered for improving concrete abrasion resistance. Details such as addition dosages and types, as well as the working mechanisms, should be explored in depth.

(5) The prediction of concrete abrasion damage is a very important subject. In general, existing empirical models are far from being adequate. Numerical modeling concerning concrete abrasion damage is only at the early stage. With no reference to more details herein, there is a lot of work to be done in this regard.

8. Summary and concluding remarks

This work provides a comprehensive review related to various aspects of the abrasion damage of concrete for hydraulic structures. The main contents include the theoretical background on concrete abrasion, test and characterization methods, abrasion prediction models, key influencing parameters, and approaches to improving concrete abrasion resistance. Besides, some remaining research gaps are also identified and discussed. Based on the review, the following conclusions can be drawn:

(1) The abrasion damage of concrete subjected to the sediment-laden flow is highly associated with energy conversion, indicating that the larger the kinetic energy, the more the abrasion material loss. The kinetic energy is highly dependent of the flow velocity and sediment contents. The increase in the flow velocity and sediment content leads to an increment in the kinetic energy transmitted by the flow and thus more abrasion material loss of concrete. During the interaction between the flow and concrete materials, there exist two types of abrasion wear mechanisms, namely impact deformation and cutting wear. The abrasion damage of concrete is a physical process of accumulated material loss during the long-term abrasion period, which can be linked closely to the crack evolution process. Based on the distance to the entry point of the sediment-laden flow, the abrasion damage of concrete for hydraulic structures may be divided into three zones, and the extent of the damage tends to decrease as the distance increases.

(2) Concrete abrasion damage can be characterized quantitatively by different performance indicator(s)/parameter(s), including abrasion mass/volume loss, abrasion depths/widths, abrasion area distributions, and abrasion rates. The combined use of those indicators may present a better description of the concerned abrasion damage.

(3) The abrasion resistance of concrete may be tested by various methods, including standard methods, waterborne sand impact methods, high-pressure hydro-abrasive jet methods, scaled physical-model test methods, and in-situ test methods.

(4) The empirical models are mainly used to estimate concrete abrasion damage. They can be applied simply to establish the relation between concrete abrasion damage and an influencing parameter. However, the influence of other influencing factors on concrete abrasion damage cannot be effectively reflected. The semi-empirical models may improve the prediction accuracy to some extent by combining experimental data and mathematical theory but require more assumptions. The probabilistic model mainly focuses on the special case so its application to other

hydraulic conditions is not convincing. The models established based on machine learning methodologies are promising to predict concrete abrasion damage. This kind of models consider most of the relevant influencing parameters according to the obtained dataset, so it can be used for comprehensive evaluation of concrete exposed to complex conditions. However, the prediction accuracy may be compromised due to the small dataset adopted.

(5) Concrete abrasion resistance is affected by a number of factors, especially hydraulic conditions and concrete properties. Important parameters include, e.g., flow velocity, flow impact angle, sediment content, abrasive particle property, exposure time, concrete strength, and concrete pore structure. However, there are large variations in the reported results concerning the effects of the parameters, indicating the complexity of the abrasion problem.

(6) A number of approaches for improving concrete abrasion resistance are discussed. It is noted that the incorporation of fibers into concrete mixtures enhances concrete abrasion resistance. However, the fiber volume fractions may not go beyond 2.5 vol%, since it may cause physical difficulties in obtaining a homogeneous distribution of the fibers in the concrete system. Supplementary cementitious materials used in concrete mixtures, e.g., fly ash, silica fume, and GGBS, may increase concrete abrasion resistance, but the reported effects are quite inconsistent and highly dependent on the types and the contents of additions. The inclusion of an appropriate amount of rubber particles can improve concrete abrasion resistance. Surface protective materials can act as a physical barrier to prevent abrasion damage of the concrete beneath if the interface bond between the protective materials and the concrete can be secured.

Last but not least, it should be highlighted that limited information exists in current design codes and recommendations concerning concrete abrasion design, which leaves the industries directionless in their work. The research work also has a limited impact on the current construction practice. From a practical and more general perspective, it may be important to emphasize that researchers may need to spend more efforts in communicating the research results to relevant stakeholders, so the state-of-the-art knowledge can be passed on. Researchers may be the best that can influence and strengthen the link between research and industry. Durable and sustainable hydraulic structures with excellent abrasion resistance may only be achieved through common efforts from both academia and industry.

CRediT authorship contribution statement

Qiong Liu: Writing – original draft, Methodology, Investigation, Formal analysis, Data curation, Conceptualization. **Lars Andersen:** Writing – review & editing, Supervision, Methodology. **Mingzhong Zhang:** Writing – review & editing, Supervision, Methodology. **Min Wu:** Writing – review & editing, Supervision, Project administration, Methodology, Funding acquisition, Formal analysis, Conceptualization.

Declaration of Competing Interest

The authors declare that they have no known competing financial interests or personal relationships that could have appeared to influence the work reported in this paper.

Data availability

Data will be made available on request.

References

[1] M. Müller-Hagmann, I. Albayrak, C. Auel, R.M. Boes, Field investigation on hydroabrasion in high-speed sediment-laden flows at sediment bypass tunnels, Water (Switz.) 12 (2020) 10–16, https://doi.org/10.3390/w12020469.

[2] A. Kryżanowski, M. Mikoš, J. Šušteršiè, V. Ukrainczyk, I. Planinc, Testing of concrete abrasion resistance in hydraulic structures on the Lower Sava River, Stroj. Vestn. -/J. Mech. Eng. 58 (2012) 245–254, https://doi.org/10.5545/sv-jme.2010.217.

[3] N. Omoding, L.S. Cunningham, G.F. Lane-Serff, M. Omer, B. Farrington, Field Investigation into abrasion of concrete at a coastal stepped revetment: A U.K. case study, J. Mar. Sci. Eng. 11 (2023) 1145, https://doi.org/10.3390/jmse11061145.

[4] B.D. Scott, M. Safiuddin, Abrasion resistance of concrete – design, construction and case study, Concr. Res. Lett. 6 (2015), https://doi.org/10.1061/(asce)0899-1561(1991)3:1(19).

[5] T.C. Liu, J.E. McDonald, Abrasion-erosion resistance of fiber-reinforced concrete, (1981).

[6] C. Auel, Flow Characteristics, Particle Motion And Invert Abrasion In Sediment Bypass Tunnels, ETH Zurich, 2014.

[7] M. Müller-Hagmann, Hydroabrasion by High-Speed Sediment-Laden Flows in Sediment Bypass Tunnels, ETH ZURICH, 2018.

[8] M. Facchini, Hydroabrasion in high speed flow at sediment bypass tunnels, ETH Zürich, 2017.

[9] The American Society for Testing and Materials, Standard Test Method for Abrasion Resistance of Concrete by Sandblasting, ASTM C418-98. (1999) 1–3.

[10] The American Society for Testing and Materials, Standard Test Method for Abrasion Resistance of Concrete (Underwater Method), ASTM C1138-97. (1997) 1–4.

[11] A.W. Momber, Effects of erodent flow energy and local exposure time on the erosion of cement-based composites at high-speed hydro-abrasive flow, 378–379, Wear (2017) 145–154, https://doi.org/10.1016/j.wear.2017.01.120.

[12] N.J. Finnegan, L.S. Sklar, T.K. Fuller, Interplay of sediment supply, river incision, and channel morphology revealed by the transient evolution of an experimental bedrock channel, J. Geophys. Res. Earth Surf. 112 (2007), https://doi.org/10.1029/2006JF000569.

[13] P. Chatanantavet, G. Parker, Experimental study of bedrock channel alluviation under varied sediment supply and hydraulic conditions, Water Resour. Res. 44 (2008), https://doi.org/10.1029/2007WR006581.

[14] M. Facchini, Downstream morphological effects ofSediment Bypass Tunnels, VAW-Mitt. 243 (2017).

[15] A. Kryżanowski, M. Mikoš, J. Šušteršiè, V. Ukrainczyk, I. Planinc, Testing of concrete abrasion resistance in hydraulic structures on the Lower Sava River, Stroj. Vestn. -J. Mech. Eng. 58 (2012) 245–254, https://doi.org/10.5545/sv-jme.2010.217.

[16] F. Jacobs, W. Winkeler, F. Hinkeler, P. Volkart, Beton Im. Wasserbau, Beton 1 (2003) 16–23.

[17] Y.W. Liu, Improving the abrasion resistance of hydraulic-concrete containing surface crack by adding silica fume, Constr. Build. Mater. 21 (2007) 972–977, https://doi.org/10.1016/j.conbuildmat.2006.03.001.

[18] R. Dandapat, A. Deb, A probability based model for the erosive wear of concrete by sediment bearing water, 350–351, Wear (2016) 166–181, https://doi.org/10.1016/j.wear.2016.01.012.

[19] S.R. Abid, M.S. Shamkhi, N.S. Mahdi, Y.H. Daek, Hydro-abrasive resistance of engineered cementitious composites with PP and PVA fiber, Constr. Build. Mater. J. 187 (2018) 168–177.

[20] E.K. Horszczaruk, Hydro-abrasive erosion of high performance fiber-reinforced concrete, Wear 267 (2009) 110–115, https://doi.org/10.1016/j.wear.2008.11.010.

[21] Z. Sun, Q. Xu, Microscopic, physical and mechanical analysis of polypropylene fiber reinforced concrete, Mater. Sci. Eng. A 527 (2009) 198–204, https://doi.org/10.1016/j.msea.2009.07.056.

[22] A. Alaskar, H. Alabduljabbar, A.M. Mohamed, F. Alrshoudi, R. Alyousefb, Abrasion and skid resistance of concrete containing waste polypropylene fibers and palm oil fuel ash as pavement material, Constr. Build. Mater. J. 282 (2021) 122681.

[23] M. Mazzuoli, G. Vittori, P. Blondeaux, The dynamics of sliding, rolling and saltating sediments in oscillatory flows, Eur. J. Mech. / B Fluids 94 (2022) 246–262.

[24] R.A. Bagnold, The nature of saltation and of "bed-load" transport in water, Proc. Roy. Soc. Lond., Ser. A 332 (1973) 473–504, https://doi.org/10.1098/rspa.1973.0038.

[25] S.K. Bose, S. Dey, Sediment entrainment probability and threshold of sediment suspension: exponential-based approach, J. Hydraul. Eng. 139 (2013) 1099–1106.

[26] J.D. Fenton, J.E. Abbott, Initial Movement of Grains on a Stream Bed: The Effect of Relative Protrusion, Proc. R. Soc. Lond. Ser. A 352 (1977) 523–537, https://doi.org/10.1098/rspa.1977.0014.

[27] C. Ancey, F. Bigillon, P. Frey, J. Lanier, R. Ducret, Saltating motion of a bead in a rapid water stream, Phys. Rev. E. 66 (2002) 036306.

[28] J.R.D. Francis, Experiments on the motion of solitary grains along the bed of a water-stream, Proc. Roy. Soc. Lond., Ser. A 332 (1973) 443–471, https://doi.org/10.1098/rspa.1973.0037.

[29] S.K. Bose, S. Dey, Sediment entrainment probability and threshold of sediment suspension: exponential based approach, J. Hydraul. Eng. 139 (2013) 1099–1106.

[30] J.E. Abbott, J.R.D. Francis, Saltation and suspension trajectories of solid grains in a water stream, Philos. Trans. R. Soc. 284 (1977) 225–254, https://doi.org/10.1098/rsta.1977.0009.

[31] Z. Wu, J. Zhang, H. Yu, H. Ma, L. Chen, W. Dong, Y. Huan, Y. Zhang, Coupling effect of strain rate and specimen size on the compressive properties of coral aggregate concrete: A 3D mesoscopic study, Compos. Part B Eng. 200 (2020), https://doi.org/10.1016/j.compositesb.2020.108299.

[32] B.S.N. Ristić, Z. Grdić, G. Topličić-Ćurčić, D. Grdić, D. Krstić, Mechanisms of hydro-abrasive damage and methods of examination of hydro-abrasive resistance of concrete in hydraulic structures, in: SFERA 2017 Tehnol. Betona, 2017: pp. 106–111.

[33] M. Mu, L. Feng, Q. Zhang, W. Zang, H. Wang, Study on abrasive particle impact modeling and cutting mechanism, Energy Sci. Eng. 10 (2022) 96–119, https://doi.org/10.1002/ese3.1012.

[34] J.H. Neilson, A. Gilchrist, Erosion by a stream of solid particles, Wear 11 (1968) 111–122, https://doi.org/10.1016/0043-1648(68)90591-7.

[35] I. Finnie, Erosion of surfaces by solid particles, Wear 3 (1960) 87–103, https://doi.org/10.1016/0043-1648(60)90055-7.

[36] L.S. Sklar, W.E. Dietrich, A mechanistic model for river incision into bedrock by saltating bed load, Water Resour. Res. 40 (2004) 1–22, https://doi.org/10.1029/2003WR002496.

[37] J.G.A. Bitter, A Study of Erosion Phenomena Part I, Wear 6 (1963) 169–190.

[38] H.M.I. Clark, K.K. Wong, Impact angle, particle energy and mass loss in erosion by dilute slurries, 186–187, Wear (1995) 454–464, https://doi.org/10.1016/0043-1648(95)07120-2.

[39] F. Qiu, J. Huang, Y. Li, Z. Han, W. Wang, G. Chen, X. Qu, B. Su, Protecting highway bridges against debris flows using lateral berms: A case study of the 2008 and 2011 Cheyang debris flow events, China, Geomat., Nat. Hazards Risk. 9 (2018) 196–210, https://doi.org/10.1080/19475705.2017.1414718.

[40] Y.W. Liu, T. Yen, T.H. Hsu, Abrasion erosion of concrete by water-borne sand, Cem. Concr. Res. 36 (2006) 1814–1820, https://doi.org/10.1016/j.cemconres.2005.03.018.

[41] S. Pyo, S.Y. Abate, H.K. Kim, Abrasion resistance of ultra high performance concrete incorporating coarser aggregate, Constr. Build. Mater. 165 (2018) 11–16, https://doi.org/10.1016/j.conbuildmat.2018.01.036.

[42] Z. Grdić, G. Topličić-ćurčić, N. Ristić, D. Grdić, P. Mitković, Hydro-abrasive resistance and mechanical properties of rubberized concrete, J. Croat. Assoc. Civ. Eng. (2014) 10–20, https://doi.org/10.14256/jce.910.2013.

[43] C. Thomas, I. Lombillo, J.A. Polanco, L. Villegas, J. Setién, M.V. Biezma, Polymeric and cementitious mortars for the reconstruction of natural stone structures exposed to marine environments, Compos. Part B Eng. 41 (2010) 663–672, https://doi.org/10.1016/j.compositesb.2010.08.007.

[44] The American Society for Testing and Materials, Standard Test Method for Abrasion Resistance of Horizontal Concrete Surfaces, ASTM C 779/C 779M - 05. (2002) 1–6.

[45] The American Society for Testing and Materials, Standard test method for abrasion resistance of concrete or mortar surfaces by the rotating-cutter method, ASTM C944-99. (1999) 1–4, https://doi.org/10.1520/mnl10913m.

[46] E. Horszczaruk, P. Brzozowski, Abrasion resistance and mechanical strength of underwater repair concrete curing under hydrostatic pressure, Constr. Build. Mater. 394 (2023), https://doi.org/10.1016/j.conbuildmat.2023.132256.

[47] I. Sosa, C. Thomas, J.A. Polanco, J. Setién, J.A. Sainz-Aja, P. Tamayo, Durability of high-performance self-compacted concrete using electric arc furnace slag aggregate and cupola slag powder, Cem. Concr. Compos, J 127 (2022) 104399.

[48] N. Zarrabi, M.N. Moghim, M.R. Eftekhar, Effect of hydraulic parameters on abrasion erosion of fiber reinforced concrete in hydraulic structures, Constr. Build. Mater. 267 (2021) 120996.

[49] Z.J. Grdic, G.A.T. Curcic, N.S. Ristic, I.M. Despotovic, Abrasion resistance of concrete micro-reinforced with polypropylene fibers, Constr. Build. Mater. 27 (2012) 305–312, https://doi.org/10.1016/j.conbuildmat.2011.07.044.

[50] H. Hocheng, C.H. Weng, Hydraulic erosion of concrete by a submerged jet, J. Mater. Eng. Perform. 11 (2002) 256–261, https://doi.org/10.1361/105994902770344033.

[51] J. Liu, S. Du, Y. Xue, Study on the breaking process and damage characteristics of abrasive water jet impacting concrete based on acoustic emission, Constr. Build. Mater. 262 (2020) 120085.

[52] T. Inoue, N. Izumi, Y. Shimizu, G. Parker, Interaction among alluvial cover, bed roughness, and incision rate in purely bedrock and alluvial-bedrock channel, J. Geophys. Res. Earth Surf. 119 (2014) 2123–2146, https://doi.org/10.1002/2014JF003133.

[53] M.P. Lamb, N.J. Finnegan, J.S. Scheingross, L.S. Sklar, New insights into the mechanics of fluvial bedrock erosion through flume experiments and theory, Geomorphology 244 (2015) 33–55, https://doi.org/10.1016/j.geomorph.2015.03.003.

[54] Q. Liu, Li, L.V. Andersen, M. Wu, Studying the abrasion damage of concrete for hydraulic structures under various flow conditions, Cem. Concr. Compos, J 135 (2023) 104849.

[55] R. Siddique, J.M. Khatib, Abrasion resistance and mechanical properties of high-volume fly ash concrete, Mater. Struct. 43 (2010) 709–718, https://doi.org/10.1617/s11527-009-9523-x.

[56] A. García, D. Castro-Fresno, J.A. Polanco, C. Thomas, Abrasive wear evolution in concrete pavements, Road. Mater. Pavement Des. 13 (2012) 534–548, https://doi.org/10.1080/14680629.2012.694094.

[57] E. Horszczaruk, P. Brzozowski, Effects of fluidal fly ash on abrasion resistance of underwater repair concrete, 376–377, Wear (2017) 15–21, https://doi.org/10.1016/j.wear.2017.01.051.

[58] Y.W. Liu, S.W. Cho, T.H. Hsu, Impact abrasion of hydraulic structures concrete, J. Mar. Sci. Technol. 20 (2012) 253–258, https://doi.org/10.51400/2709-6998.1801.

[59] L. Sitek, P. Hlaváček, L. Bodnárová, Use of high-speed water flows for accelerated mechanical modelling of erosive wear of concrete surfaces, MATEC Web Conf. 244 (2018), https://doi.org/10.1051/matecconf/201824402007.

[60] A. Momber, R. Kovacevic, Fundamental investigations on concrete wear by high velocity water flow, Wear 177 (1994) 55–62, https://doi.org/10.1016/0043-1648(94)90117-1.

[61] M. Woldman, E. van der Heide, D.J. Schipper, T. Tinga, M.A. Masen, Investigating the influence of sand particle properties on abrasive wear behaviour, 294–295, Wear (2012) 419–426, https://doi.org/10.1016/j.wear.2012.07.017.

[62] A. Kryžanowski, M. Mikoš, J. Šušteršic, I. Planinc, Abrasion resistance of concrete in hydraulic structures, Acids Mater. J. 106 (2009) 349–356, https://doi.org/10.14359/56655.

[63] J.P. Johnson, K.X. Whipple, Feedbacks between erosion and sediment transport in experimental bedrock channels, Earth Surf. Process. Landf. 32 (2007) 1048–1062, https://doi.org/10.1002/esp.1471.

[64] A.F.H. Sherwani, R. Faraj, K.H. Younis, A. Daraei, Strength, abrasion resistance and permeability of artificial fly-ash aggregate pervious concrete, Case Stud. Constr. Mater. 14 (2021) e00502, https://doi.org/10.1016/j.cscm.2021.e00502.

[65] E. Horszczaruk, Abrasion resistance of high-strength concrete in hydraulic structures, Wear 259 (2005) 62–69, https://doi.org/10.1016/j.wear.2005.02.079.

[66] T. Yen, T.H. Hsu, Y.W. Liu, S.H. Chen, Influence of class F fly ash on the abrasion-erosion resistance of high-strength concrete, Constr. Build. Mater. 21 (2007) 458–463, https://doi.org/10.1016/j.conbuildmat.2005.06.051.

[67] R. Siddique, K. Kapoor, E.H. Kadri, R. Bennacer, Effect of polyester fibres on the compressive strength and abrasion resistance of HVFA concrete, Constr. Build. Mater. 29 (2012) 270–278, https://doi.org/10.1016/j.conbuildmat.2011.09.011.

[68] Q. Deng, R. Zhang, C. Liu, Z. Duan, J. Xiao, Influence of fiber properties on abrasion resistance of recycled aggregate concrete: Length, volume fraction, and types of fibers, Constr. Build. Mater. 362 (2023) 129750.

[69] X.G. Hu, A.W. Momber, Y. Yin, H. Wang, D.M. Cui, High-speed hydrodynamic wear of steel-fibre reinforced hydraulic concrete, Wear 257 (2004) 441–450, https://doi.org/10.1016/j.wear.2004.01.019.

[70] X. Wang, S.Z. Luo, Y.A. Hu, Q. Yuan, H.S. Wang, L.H. Zhao, High-speed flow erosion on a new roller compacted concrete dam during construction, J. Hydrodyn. 24 (2012) 32–38, https://doi.org/10.1016/S1001-6058(11)60216-3.

[71] X. Hu, A.W. Momber, Y. Yin, Hydro-abrasive erosion of steel-fibre reinforced hydraulic concrete, Wear 253 (2002) 848–854, https://doi.org/10.1002/best.200303060.

[72] J.G.A. Bitter, A study of erosion phenomena part II, Wear 6 (1963) 5–21, https://doi.org/10.1016/0043-1648(63)90003-6.

[73] Michael G. Foley, Bedrock incision by streams, Geol. Soc. Am. Bull. 91 (1980) 2189–2213.

[74] T. Ishibashi, A hydraulic study on protection for erosion of sediment flush equipments of dams, Proc. Jpn. Soc. Civ. Eng. 334 (1983) 103–112.

[75] W.J. Head, M.E. Harr, The development of a model to predict the erosion of materials by natural contaminants, Wear 15 (1970) 1–46, https://doi.org/10.1016/0043-1648(70)90184-5.

[76] O. Gencel, F. Kocabas, M.S. Gok, F. Koksal, Comparison of artificial neural networks and general linear model approaches for the analysis of abrasive wear of concrete, Constr. Build. Mater. 25 (2011) 3486–3494, https://doi.org/10.1016/j.conbuildmat.2011.03.040.

[77] N. Najimi, M. Sobhani, Modelling the abrasion resistance of self-consolidating concrete, Mag. Concr. Res. 67 (2015) 938–953.

[78] S. Malazdrewicz, Ł. Sadowski, An intelligent model for the prediction of the depth of the wear of cementitious composite modified with high-calcium fly ash, Compos. Struct. J. 259 (2021) 113234.

[79] S. Malazdrewicz, Ł. Sadowski, Neural modelling of the depth of wear determined using the rotating-cutter method for concrete with a high volume of high-calcium fly ash, Wear 477 (2021) 203791.

[80] Q. Liu, L.V. Andersen, M. Wu, Prediction of concrete abrasion depth and computational design optimization of concrete mixtures, Cem. Concr. Compos. (2024) 105431.

[81] R. Siddique, Performance characteristics of high-volume Class F fly ash concrete, Cem. Concr. Res. 34 (2004) 487–493, https://doi.org/10.1016/j.cemconres.2003.09.002.

[82] T.R. Naik, S.S. Singh, M.M. Hossain, Abrasion resistance of concrete as influenced by inclusion of fly ash, Cem. Concr. Res. 24 (1994) 303–312, https://doi.org/10.1016/0008-8846(94)90056-6.

[83] I. Yoshitake, S. Ueno, Y. Ushio, H. Arano, S. Fukumoto, Abrasion and skid resistance of recyclable fly ash concrete pavement made with limestone aggregate, Constr. Build. Mater. 112 (2016) 440–446.

[84] M. Sharbaf, M. Najimi, N. Ghafoori, A comparative study of natural pozzolan and fly ash: Investigation on abrasion resistance and transport properties of self-consolidating concrete, Constr. Build. Mater. 346 (2022) 128330.

[85] G. Singh, R. Siddique, Abrasion resistance and strength properties of concrete containing waste foundry sand (WFS), Constr. Build. Mater. 28 (2012) 421–426, https://doi.org/10.1016/j.conbuildmat.2011.08.087.

[86] T.M. Oh, G.C. Cho, Characterization of Effective Parameters in Abrasive Waterjet Rock Cutting, Rock. Mech. Rock. Eng. 47 (2014) 745–756.

[87] M. Curbach, J. Eibl, Crack velocity in concrete, Eng. Fract. Mech. 35 (1990) 321–326, https://doi.org/10.1016/0013-7944(90)90210-8.

[88] E. Horszczaruk, The model of abrasive wear of concrete in hydraulic structures, Wear 256 (2004) 787–796, https://doi.org/10.1016/S0043-1648(03)00525-8.

[89] X. Wang, T. Xie, Cavitation erosion behavior of hydraulic concrete under high-speed flow, Anti-Corros. Methods Mater. 70 (2022) 81–93.

[90] C. Liu, Z. Li, S. Fu, L. Ding, G. Wu, Influence of soil aggregate characteristics on the sediment transport capacity of overland flow, Geoderma 369 (2020), https://doi.org/10.1016/j.geoderma.2020.114338.

[91] N. Izumi, M. Yokokawa, G. Parker, Incisional cyclic steps of permanent form in mixed bedrock-alluvial rivers, J. Geophys. Res. Earth Surf. Res. 122 (2017) 130–152.

[92] G.K. Gilbert, Report of the geology of the Henry Mountains, geographical and geological survery of the Rocky Mountain Region: Government Printing Office, Washingt. DC. (1877).

[93] L.A. Leonard, M.E. Luther, Flow hydrodynamics in tidal marsh canopies, Limnol. Oceanogr. 40 (1995) 1474–1484, https://doi.org/10.4319/lo.1995.40.8.1474.

[94] L. Sklar, W.E. Dietrich, River longitudinal profiles and bedrock incision models: Stream power and the influence of sediment supply, in: Geophys. Monogr. Geophys. Union, AGU AMERICAN GEOPHYSICAL UNION, 1998: pp. 237–260.

[95] G.R. Kumar, U.K. Sharma, Standard test methods for determination of abrasion resistance of concrete, Int. J. Civ. Eng. Res 5 (2014) 155–162.

[96] F. Wu, Q. Yu, X. Chen, Effects of steel fibre type and dosage on abrasion resistance of concrete against debris flow, Cem. Concr. Compos. 134 (2022), https://doi.org/10.1016/j.cemconcomp.2022.104776.

[97] R. Kunterding, Beanspruchung der Oberfläche von Stahlbetonsilos durch Schüttgüter ('Surface stress of concrete silos due to bulk solids'), 1991.

[98] X. Cai, Z. He, S. Tang, X. Chen, Abrasion erosion characteristics of concrete made with moderate heat Portland cement, fly ash and silica fume using sandblasting test, Constr. Build. Mater. J. 127 (2016) 804–814.

[99] J.M. Turowski, Stochastic modeling of the cover effect and bedrock erosion Jens, Water Resour. Res. 45 (2009), https://doi.org/10.1029/2008WR007262.

[100] T.R. Bajracharya, B. Acharya, C.B. Joshi, R.P. Saini, O.G. Dahlhaug, Sand erosion of Pelton turbine nozzles and buckets: A case study of Chilime Hydropower Plant, Wear 264 (2008) 177–184, https://doi.org/10.1016/j.wear.2007.02.021.

[101] R. Okita, Y. Zhang, B.S. McLaury, S.A. Shirazi, Experimental and computational investigations to evaluate the effects of fluid viscosity and particle size on erosion damage, J. Fluids Eng. 134 (2012), 061301–061301.

[102] M. Attal, P.A. Cowie, A.C. Whittaker, D. Hobley, G.E. Tucker, G.P. Roberts, Testing fluvial erosion models using the transient response of bedrock rivers to tectonic forcing in the Apennines, Italy, J. Geophys. Res. Earth Surf. 116 (2011), https://doi.org/10.1029/2010JF001875.

[103] A.R. Beer, J.M. Turowski, Bedload transport controls bedrock erosion under sediment-starved conditions, Earth Surf. Dyn. 3 (2015) 291–309, https://doi.org/10.5194/esurf-3-291-2015.

[104] H. Hertz, Ueber die Berührung fester elastischer Körper, J. Fur Die Reine Und Angew. Math. (92) (1881) 156–171, https://doi.org/10.1515/crll.1882.92.156.

[105] S. Fabbro, L.M. Araujo, J. Engel, J. Kondratiuk, M. Kuffa, K. Wegener, Abrasive and adhesive wear behaviour of metallic bonds in a synthetic slurry test for wear prediction in reinforced concrete, Wear 476 (2021) 203690.

[106] D.W.E. Sklar, Sediment and rock strength controls on river incision into bedrock, Geology 29 (2001) 1087–1090.

[107] T. Bovet, Contribution à l'étude du phénomène d'érosion par frottement dans le domaine des turbines hydrauliques, Bull. Tech. La Suisse Rom. 3 (1958) 3–15.

[108] L. Beixing, K. Guoju, Z. Mingkai, Influence of manufactured sand characteristics on strength and abrasion resistance of pavement cement concrete, Constr. Build. Mater. J. 25 (2011) 3849–3853.

[109] S.K. Rao, P. Sravana, T.C. Rao, Abrasion resistance and mechanical properties of Roller Compacted Concrete with GGBS, Constr. Build. Mater. 114 (2016) 925–933.

[110] M. Sonebi, K.H. Khayat, Testing abrasion resistance of high-strength concrete, Cem. Concr. Aggreg. 23 (2001) 34–43.

[111] A.M. Rashad, A preliminary study on the effect of fine aggregate replacement with metakaolin on strength and abrasion resistance of concrete, Constr. Build. Mater. 44 (2013) 487–495.

[112] I. Papayianni, E. Anastasiou, Production of high-strength concrete using high volume of industrial by-products, Constr. Build. Mater. 24 (2010) 1412–1417, https://doi.org/10.1016/j.conbuildmat.2010.01.016.

[113] Q. Qin, Q. Meng, H. Yang, W. Wud, Study of the anti-abrasion performance and mechanism of coral reef sand concrete, Constr. Build. Mater. 291 (2021) 123263.

[114] J. Leon Raj, T. Chockalingam, Strength and abrasion characteristics of pervious concrete, Road. Mater. Pavement Des. 21 (2020) 2180–2197, https://doi.org/10.1080/14680629.2019.1596828.

[115] Y. Liu, Y. Wei, Abrasion resistance of ultra-high performance concrete with coarse aggregate, Mater. Struct. 54 (2021), https://doi.org/10.1617/s11527-021-01750-6.

[116] E.E. Small, T. Blom, G.S. Hancock, B.M. Hynek, C.W. Wobus, Variability of rock erodibility in bedrock-floored stream channels based on abrasion mill experiments, J. Geophys. Res. Earth Surf. 120 (2015) 1455–1469, https://doi.org/10.1002/2015JF003506.

[117] V. Mechtcherine, C. Bellmann, U. Helbig, H.B. Horlacher, J. Stamm, Nachbildung der Hydroabrasionsbeanspruchung im Laborversuch Teil 1 – Experimentelle Untersuchungen zu Schädigungsmechanismen im Beton, Bautechnik 89 (2012) 309–319.

[118] E. Horszczaruk, Mathematical model of abrasive wear of high performance concrete, Wear 264 (2008) 113–118, https://doi.org/10.1016/j.wear.2006.12.008.

[119] C.D. Atis, O.N. Çelik, Relation between abrasion resistance and flexural strength of high volume fly ash concrete, Mater. Struct. Constr. 34 (2002) 257–260, https://doi.org/10.1007/bf02533087.

[120] M. Gupta, M. Kumar, Effect of nano silica and coir fiber on compressive strength and abrasion resistance of concrete, Constr. Build. Mater. 226 (2019) 44–50, https://doi.org/10.1016/j.conbuildmat.2019.07.232.

[121] C. Auel, I. Albayrak, T. Sumi, R.M. Boes, Sediment transport in high-speed flows over a fixed bed: 1. Particle dynamics, Earth Surf. Process. Landf. 42 (2017) 1365–1383.

[122] N. Fonseca, J. de Brito, L. Evangelista, The influence of curing conditions on the mechanical performance of concrete made with recycled concrete waste, Cem. Concr. Compos. J. 33 (2011) 637–643, https://doi.org/10.1080/00218464.2019.1656615.

[123] S.K. Rao, P. Sravana, T.C. Rao, Investigating the effect of M-sand on abrasion resistance of Fly Ash Roller Compacted Concrete (FRCC), Constr. Build. Mater. 122 (2016) 191–201, https://doi.org/10.1016/j.conbuildmat.2016.06.054.

[124] A.M. Rashad, H.E.D.H. Seleem, A.F. Shaheen, Effect of silica fume and slag on compressive strength and abrasion resistance of HVFA concrete, Int. J. Concr. Struct. Mater. 8 (2014) 69–81, https://doi.org/10.1007/s40069-013-0051-2.

[125] M. Uysal, The influence of coarse aggregate type on mechanical properties of fly ash additive self-compacting concrete, Constr. Build. Mater. 37 (2012) 533–540, https://doi.org/10.1016/j.conbuildmat.2012.07.085.

[126] T. Gupta, S.N. Sachdeva, Laboratory investigation and modeling of concrete pavements containing AOD steel slag, Cem. Concr. Res. 124 (2019) 105808.

[127] L. Wang, S.H. Zhou, Y. Shi, S.W. Tang, E. Chen, Effect of silica fume and PVA fiber on the abrasion resistance and volume stability of concrete, Compos. Part B Eng. 130 (2017) 28–37, https://doi.org/10.1016/j.compositesb.2017.07.058.

[128] N. Saikia, J. de Brito, Mechanical properties and abrasion behaviour of concrete containing shredded PET bottle waste as a partial substitution of natural aggregate, Constr. Build. Mater. 52 (2014) 236–244.

[129] K. Ueno, S. Takahashi, M. Yamamoto, T. Kanamori, S. Kawabe, I. Nakajima, M. Ishii, Influences of test conditions of sandblasting on replicability of abrasion pattern of concrete subjected to hydrodynamic action, Case Stud. Constr. Mater. 18 (2023) e01812.

[130] C.D. Atis, High volume fly ash abrasion resistant concrete, J. Mater. Civ. Eng. 14 (2002) 274–277.

[131] P. Laplante, P.C. Aitcin, D. Vezina, Abrasion resistance of concrete, J. Mater. Civ. Eng. 3 (1991) 19–28.

[132] M.K. Ismail, A.A.A. Hassan, Abrasion and impact resistance of concrete before and after exposure to freezing and thawing cycles, Constr. Build. Mater. 215 (2019) 849–861.

[133] J.S. Scheingross, F. Brun, D.Y. Lo, K. Omerdin, M.P. Lamb, Experimental evidence for fluvial bedrock incision by suspended and bedload sediment, Geology 42 (2014) 523–526, https://doi.org/10.1130/G35432.1.

[134] A. Kiliç, C.D. Atiş, A. Teymen, O. Karahan, F. Özcan, C. Bilim, M. Özdemir, The influence of aggregate type on the strength and abrasion resistance of high strength concrete, Cem. Concr. Compos. 30 (2008) 290–296, https://doi.org/10.1016/j.cemconcomp.2007.05.011.

[135] X. Qin, J. Guo, C. Gu, X. Chen, B. Xu, A discrete-continuum coupled numerical method for fracturing behavior in concrete dams considering material heterogeneity, Constr. Build. Mater. 305 (2021), https://doi.org/10.1016/j.conbuildmat.2021.124741.

[136] N. Omoding, L.S. Cunningham, G.F. Lane-Serff, Influence of Coarse Aggregate Parameters and Mechanical Properties on the Abrasion Resistance of Concrete in Hydraulic, Struct., J. Mater. Civ. Eng. 33 (2021) 04021244.

[137] N.F. Medina, D.F. Medina, F. Hernández-Olivares, M.A. Navacerrada, Mechanical and thermal properties of concrete incorporating rubber and fibres from tyre recycling, Constr. Build. Mater. 144 (2017) 563–573.

[138] Q. Qin, Q. Meng, H. Yang, W. Wu, Study of the anti-abrasion performance and mechanism of coral reef sand concrete, Constr. Build. Mater. 291 (2021) 123263, https://doi.org/10.1016/j.conbuildmat.2021.123263.

[139] H.A. Ibrahim, H. Abdul Razak, F. Abutaha, Strength and abrasion resistance of palm oil clinker pervious concrete under different curing method, Constr. Build. Mater. 147 (2017) 576–587, https://doi.org/10.1016/j.conbuildmat.2017.04.072.

[140] P. Richard, M.H. Cheyrezy, Reactive powder concretes with high ductility and 200–800 MPa compressive strength, Spec, Publ 144 (1994) 507–518.

[141] L. Wang, M. Jin, F. Guo, Y.A.N. Wang, S. Tang, Pore structural and fractal analysis of the influence of fly ash and silica fume on the mechanical property and abrasion resistance of concrete, Fractals 29 (2021), https://doi.org/10.1142/S0218348×2140003X.

[142] T. Li, X. Liu, Z. Wei, Y. Zhao, D. Yan, Study on the wear-resistant mechanism of concrete based on wear theory, Constr. Build. Mater. 271 (2021) 121594.

[143] C.T.I. Sosa, J.A. Polanco, J. Setién, J.A. Sainz-Aja, P. Tamayo, Durability of high-performance self-compacted concrete using electric arc furnace slag aggregate and cupola slag powder, Cem. Concr. Compos. 127 (2022) 104399.

[144] J.S. Yeo, S. Koting, C.C. Onn, K.H. Mo, An overview on the properties of eco-friendly concrete paving blocks incorporating selected waste materials as aggregate, Environ. Sci. Pollut. Res. (2021) https://doi.org/10.1007/s11356-021-13836-3.

[145] S.V. Joshi, L.T. Drzal, A.K. Mohanty, S. Arora, Are natural fiber composites environmentally superior to glass fiber reinforced composites? Compos. Part A

Appl. Sci. Manuf. 35 (2004) 371–376, https://doi.org/10.1016/j.compositesa.2003.09.016.

[146] S.R. Abid, A.N. Hilo, N.S. Ayoob, Y.H. Daek, Underwater abrasion of steel fiber-reinforced self-compacting concrete, Case Stud. Constr. Mater. 11 (2019) e00299.

[147] O.Y. Bayraktar, G. Kaplan, J. Shi, A. Benli, B. Bodur, M. Turkoglu, The effect of steel fiber aspect-ratio and content on the fresh, flexural, and mechanical performance of concrete made with recycled fine aggregate, Constr. Build. Mater. 368 (2023) 130497.

[148] B. Felekoğlu, S. Türkel, Y. Altuntaş, Effects of steel fiber reinforcement on surface wear resistance of self-compacting repair mortars, Cem. Concr. Compos. 29 (2007) 391–396, https://doi.org/10.1016/j.cemconcomp.2006.12.010.

[149] Y.W. Liu, Y.Y. Lin, S.W. Cho, Abrasion behavior of steel-fiber-reinforced concrete in hydraulic structures, Appl. Sci. 10 (2020), https://doi.org/10.3390/app10165562.

[150] Z.Q. Shi, D.D.L. Chung, Improving the abrasion resistance of mortar by adding latex and carbon fibers, Cem. Concr. Res. 27 (1997) 1149–1153, https://doi.org/10.1016/S0008-8846(97)00097-5.

[151] P. Nuaklong, A. Wongsa, K. Boonserm, C. Ngohpok, P. Jongvivatsakul, V. Sata, P. Sukontasukkul, P. Chindaprasirt, Enhancement of mechanical properties of fly ash geopolymer containing fine recycled concrete aggregate with micro carbon fiber, J. Build. Eng. J. 41 (2021) 102403.

[152] N. Kabay, Abrasion resistance and fracture energy of concretes with basalt fiber, Constr. Build. Mater. 50 (2014) 95–101, https://doi.org/10.1016/j.conbuildmat.2013.09.040.

[153] J. Wang, R. Zhang, L. Lu, Q. Luo, X. Li, Y. Yi, X. Bai, Evaluation of mechanical properties and abrasion resistance of PAN fiber-reinforced sulfoaluminate cement composites, Case Stud. Constr. Mater. 18 (2023) e01973.

[154] S.A. Yildizel, O. Timur, A.U. Ozturk, Abrasion Resistance and Mechanical Properties of Waste-Glass-Fiber-Reinforced Roller-compacted Concrete, Mech. Compos. Mater. 54 (2018) 251–256, https://doi.org/10.1007/s11029-018-9736-6.

[155] T. Gupta, R.K. Sharma, S. Chaudhary, Influence of waste tyre fibers on strength, abrasion resistance and carbonation of concrete, Sci. Iran. 22 (2015) 1481–1489.

[156] S. Choudhary, S. Chaudhary, A. Jain, R. Gupta, Valorization of waste rubber tyre fiber in functionally graded concrete, Mater. Today Proc. 32 (2020) 645–650, https://doi.org/10.1016/j.matpr.2020.03.122.

[157] M.B. Bankir, U.K. Sevim, Performance optimization of hybrid fiber concrete according to mechanical properties, Constr. Build. Mater. J. 261 (2020) 119952.

[158] G. Araya-Letelier, F.C. Antico, M. Carrasco, P. Rojas, C.M. García-Herrera, Effectiveness of new natural fibers on damage-mechanical performance of mortar, Constr. Build. Mater. J. 152 (2017) 672–682.

[159] B. Raj, D. Sathyan, M.K. Madhavan, A. Raj, Mechanical and durability properties of hybrid fiber reinforced foam concrete, Constr. Build. Mater. 245 (2020) 118373, https://doi.org/10.1016/j.conbuildmat.2020.118373.

[160] H. Zhong, M. Zhang, Effect of recycled tyre polymer fibre on engineering properties of sustainable strain hardening geopolymer composites, Cem. Concr. Compos, J 122 (2021) 104167.

[161] Y. Liu, C. Shi, Z. Zhang, N. Li, D. Shi, Mechanical and fracture properties of ultra-high performance geopolymer concrete: Effects of steel fiber and silica fume, Cem. Concr. Compos. 112 (2020) 103665.

[162] C. Redon, V.C. Li, C. Wu, H. Hoshiro, T. Saito, A. Ogawa, Measuring and modifying interface properties of PVA fibers in ECC matrix, J. Mater. Civ. Eng. 13 (2001) 399–406.

[163] H.R. Pakravan, M. Jamshidi, M. Latifi, Investigation on polymeric fibers as reinforcement in cementitious composites: Flexural performance, J. Ind. Text. 42 (2012) 3–18, https://doi.org/10.1177/1528083711421358.

[164] R. Merli, M. Preziosi, A. Acampora, M.C. Lucchetti, E. Petrucci, Recycled fibers in reinforced concrete: A systematic literature review, J. Clean. Prod. 248 (2020) 119207.

[165] M. Khan, M. Ali, Effectiveness of hair and wave polypropylene fibers for concrete roads, Constr. Build. Mater. 166 (2018) 581–591, https://doi.org/10.1016/j.conbuildmat.2018.01.167.

[166] A. Alaskar, H. Alabduljabbar, A.M. Mohamed, F. Alrshoudi, R. Alyousefb, Abrasion and skid resistance of concrete containing waste polypropylene fibers and palm oil fuel ash as pavement material, Constr. Build. Mater. 282 (2021) 122681.

[167] L.A. Pereira De Oliveira, J.P. Castro-Gomes, Physical and mechanical behaviour of recycled PET fibre reinforced mortar, Constr. Build. Mater. 25 (2011) 1712–1717, https://doi.org/10.1016/j.conbuildmat.2010.11.044.

[168] J. Ahmad, A. Majdi, A. Al-Fakih, A.F. Deifalla, F. Althoey, M.H. El Ouni, M.A. El-Shorbagy, Mechanical and Durability Performance of Coconut Fiber Reinforced Concrete: A State-of-the-Art Review, Mater. (Basel) 15 (2022), https://doi.org/10.3390/ma15103601.

[169] M.C.G. Juenger, R. Snellings, S.A. Bernal, Supplementary cementitious materials: New sources, characterization, and performance insights, Cem. Concr. Res. 122 (2019) 257–273.

[170] B. Lothenbach, K. Scrivener, R.D. Hooton, Supplementary cementitious materials, Cem. Concr. Res. 41 (2011) 1244–1256.

[171] R. Choudhary, R. Gupta, R. Nagar, A. Jain, Mechanical and abrasion resistance performance of silica fume, marble slurry powder, and fly ash amalgamated high strength self-consolidating concrete, Constr. Build. Mater. 269 (2021) 121282.

[172] A. Aghaeipour, M. Madhkhan, Effect of ground granulated blast furnace slag (GGBFS) on RCCP durability, Constr. Build. Mater. 141 (2017) 533–541, https://doi.org/10.12989/cac.2019.23.2.133.

[173] H. Li, M. hua Zhang, J. ping Ou, Abrasion resistance of concrete containing nano-particles for pavement, Wear 260 (2006) 1262–1266, https://doi.org/10.1016/j.wear.2005.08.006.

[174] D.Z. Grdić, G.A. Topličić-ćurčić, Z.J. Grdić, N.S. Ristić, Durability properties of concrete supplemented with recycled crt glass as cementitious material, Mater. (Basel) 14 (2021), https://doi.org/10.3390/ma14164421.

[175] R. Siddique, K. Singh, P. Kunal, M. Singh, V. Corinaldesi, A. Rajor, Properties of bacterial rice husk ash concrete, Constr. Build. Mater. 121 (2016) 112–119, https://doi.org/10.1016/j.conbuildmat.2016.05.146.

[176] K. Amini, H. Ceylan, P.C. Taylor, Effect of finishing practices on surface structure and salt-scaling resistance of concrete, Cem. Concr. Compos. 104 (2019) 103345.

[177] K. Aminia, P. Vosoughi, H. Ceylan, P. Taylora, Linking air-void system and mechanical properties to salt-scaling resistance of concrete containing slag cement, Cem. Concr. Compos, J 104 (2019) 103364.

[178] X. Liu, T. Li, W. Tian, Y. Wang, Y. Chen, Study on the durability of concrete with FNS fine aggregate, J. Hazard. Mater. 381 (2020), https://doi.org/10.1016/j.jhazmat.2019.120936.

[179] R. Siddique, Effect of fine aggregate replacement with Class F fly ash on the abrasion resistance of concrete, Cem. Concr. Res. 33 (2003) 1877–1881, https://doi.org/10.1016/S0008-8846(03)00212-6.

[180] R.K. Dhir, M.R. Jones, Development of chloride-resisting concrete using fly ash, Fuel 78 (1999) 137–142, https://doi.org/10.1016/S0016-2361(98)00149-5.

[181] P. Suraneni, L. Burris, C.R. Shearer, R.D. Hooton, ASTM C618 Fly Ash Specification: Comparison with Other Specifications, Shortcomings, and Solutions, Acids Mater. J. 118 (2021) 51725994.

[182] A.M. Onaizi, N.H.A.S. Lim, G.F. Huseien, M. Amran, C.K. Ma, Effect of the addition of nano glass powder on the compressive strength of high volume fly ash modified concrete, Mater. Today Proc. 48 (2021) 1789–1795, https://doi.org/10.1016/j.matpr.2021.08.347.

[183] P.J. Tikalsky, P.M. Carrasquillo, R.L. Carrasquillo, Strength and durability considerations affecting mix proportioning of concrete containing fly ash, Mater, J 85 (1988) 505–511.

[184] S. Caliskan, Aggregate/mortar interface: influence of silica fume at the micro- and macro-level, Cem. Concr. Compos, J 25 (2003) 557–564.

[185] E. Ozbay, M. Lachemi, U.K. Sevim, Compressive strength, abrasion resistance and energy absorption capacity of rubberized concretes with and without slag, Mater. Struct. Constr. 44 (2011) 1297–1307, https://doi.org/10.1617/s11527-010-9701-x.

[186] Z. He, X. Chen, X. Cai, Influence and mechanism of micro/nano-mineral admixtures on the abrasion resistance of concrete, Constr. Build. Mater. 197 (2019) 91–98.

[187] B.S. Thomas, S. Kumar, P. Mehra, R.C. Gupta, M. Joseph, L.J. Csetenyi, Abrasion resistance of sustainable green concrete containing waste tire rubber particles, Constr. Build. Mater. 124 (2016) 906–909.

[188] M. Gesoglu, E. Güneyisi, G. Khoshnaw, S. Ipek, Abrasion and freezing–thawing resistance of pervious concretes containing waste rubbers, Constr. Build. Mater. J. 73 (2014) 19–24.

[189] S. Zhai, G. Liu, B. Pang, C. Liu, Z. Zhang, L. Zhang, L. Liu, Y. Yang, Z. Liu, Y. Zhang, Investigation on the influence of modified waste rubber powder on the abrasion resistance of concrete, Constr. Build. Mater. 357 (2022) 129409.

[190] T. Gupta, S. Chaudhary, R.K. Sharma, Assessment of mechanical and durability properties of concrete containing waste rubber tire as fine aggregate, Constr. Build. Mater. 73 (2014) 562–574, https://doi.org/10.24200/sci.2018.20334.

[191] P.K. Dehdezi, S. Erdem, M.A. Blankson, Physico-mechanical, microstructural and dynamic properties of newly developed artificial fly ash based lightweight aggregate e Rubber concrete composite, Compos. Part B Eng. 79 (2015) 451–455.

[192] Q. Han, Y. Yang, J. Zhang, J. Yu, D. Hou, B. Dong, H. Ma, Insights into the interfacial strengthening mechanism of waste rubber/cement paste using polyvinyl alcohol: Experimental and molecular dynamics study, Cem. Concr. Compos. 114 (2020) 103791.

[193] S.M.A. Qaidi, Y.Z. Dinkha, J.H. Haido, M.H. Ali, B.A. Tayeh, Engineering properties of sustainable green concrete incorporating eco-friendly aggregate of crumb rubber: A review, J. Clean. Prod. 324 (2021) 129251.

[194] F. Wu, X. Chen, J. Chen, Abrasion resistance enhancement of concrete using surface treatment methods, Tribol. Int. 179 (2023), https://doi.org/10.1016/j.triboint.2022.108180.

[195] J. Magnusson, M. Hallgren, A. Ansell, Air-blast-loaded, high-strength concrete beams. Part I: Experimental investigation, Mag. Concr. Res. 62 (2010) 127–136.

[196] X.F. Wang, Z.J. Yang, J.R. Yates, A.P. Jivkov, C. Zhang, Monte Carlo simulations of mesoscale fracture modelling of concrete with random aggregates and pores, Constr. Build. Mater. 75 (2015) 35–45, https://doi.org/10.1016/j.conbuildmat.2014.09.069.

[197] X. Zhu, Y. Bai, X. Chen, Z. Tian, Y. Ning, Evaluation and prediction on abrasion resistance of hydraulic concrete after exposure to different freeze-thaw cycles, Constr. Build. Mater. 316 (2022) 126055.

[198] S. Gupta, H.W. Kua, S.D. Pang, Effect of biochar on mechanical and permeability properties of concrete exposed to elevated temperature, Constr. Build. Mater. 234 (2020), https://doi.org/10.1016/j.conbuildmat.2019.117338.

[199] A.S. El-Dieb, D.M. Kanaan, Ceramic waste powder an alternative cement replacement – Characterization and evaluation, Sustain. Mater. Technol. 17 (2018), https://doi.org/10.1016/j.susmat.2018.e00063.